



Norwegian University  
of Life Sciences

**Master's Thesis 2022 30 ECTS**

Faculty of Environmental Sciences and Natural Resource Management

# **Testing a Fundamental Assumption in Radiation Exposure Assessments – A Study of $^{137}\text{Cs}$ Dose in Norwegian Reindeer**

Edda Bæk

Environment and Natural Resources

## Acknowledgement

With this thesis I finish my five-year university education. My two years at NMBU has been very informative and given me much joy. I have learnt about so many important things I look forward to putting into practice.

First, I want to thank my supervisors, Ole Christian Lind (NMBU), Thomas G. Hinton (Fukushima University, NMBU), and James Beasley (University of Georgia), for guiding me through the process of writing this master's thesis. Thanks for all your feedback, suggestions, and answers to my many questions, and for introducing me to an interesting field of research. I am very grateful! Also, thanks to Roar Økseter and Richard Bischof, for their time helping me out with QGIS and RStudio. Thanks to Vikas C. Baranwal, Justin Brown, and Håvard Thørring for answering questions and sharing knowledge. A special thanks to Vikas c. Baranwal at NGU for providing updated  $^{137}\text{Cs}$ -maps. I thank everyone contributing to the field work in 2019 resulting in the data used in my thesis, especially Lavrans Skuterud, Brit Salbu, Knut Hove, Marit Pettersen, and Kaveh Nikouee.

I want to thank my family and friends for all the motivation and cheering. A special thanks to Georg for his patience and support, and for offering his programming skills to help me process and analyse my data. Also, I thank my brother Sindre, for proofreading a text way out of his field of knowledge. Finally, a huge thanks to everyone at “kjelleren på Jord” for all the talks, walks, and breaks.

Norwegian University of Life Sciences (NMBU)

Ås, 16<sup>th</sup> of May 2022

Edda Bæk

## Abstract

Measuring external contaminant exposure in free-ranging animals is challenging, because of lacking adequate contaminant monitors. Therefore, most wildlife contaminant exposure data are obtained from computer simulation models, like ERICA Tool. However, assumptions used and estimates from models are rarely verified, because of the lack of empirical exposure data. Also, the spatial heterogeneous distribution of radionuclides and the temporal use of habitats by organisms complicate dosimetry simulations. Validation tests of dosimetry models are important for protecting the environment, as they are a core component of ecological risk assessments.

We wanted to test if 1) ERICA estimates of individual external dose based on mean soil contaminant concentrations are conservative, and 2) accounting for the spatial-temporal heterogeneity improves dose estimates. We compared external  $^{137}\text{Cs}$  dose rates obtained from ERICA Tool with empirical data collected using GPS-coupled contaminant monitors on three semi-domesticated reindeer grazing in the Chernobyl fallout affected mountainous Jotunheimen area, central parts of Southern Norway. Accumulated dose readings and satellite coordinates were obtained on an hourly basis for a period of 5 months. GPS locations were used to define home range and core area for the three individuals. Airborne radiometric survey data on radionuclide concentrations in soil were used to calculate mean soil contaminant concentration in the whole reindeer herding area (grand mean) and area-weighted means for home ranges and core areas. Dose rates were estimated using both grand mean and area-weighted means. We found that modelled estimations using grand mean did not result in a conservative estimate, it under-predicted external  $^{137}\text{Cs}$  dose rates in reindeer by 70% on average. Using area-weighted means to account for the spatial-temporal heterogeneity improved the estimates somewhat, but there were still under-predictions of 53% and 46% for area-weighted means for home range and core area, respectively. Thus, simulated dose rates using data reflecting central tendencies in contaminant concentrations might misguide risk assessors.

The active dosimeters provided information about variation in dose, giving us the opportunity to briefly look into the potential of using reindeer to map contaminants, by checking for correlations between dose rates and  $^{137}\text{Cs}$  concentrations in soil. The results showed some correlation ( $r_s=0.51$  on average), but data with higher dose rate values and radionuclide concentrations are needed to obtain more reliable results. Future research should focus on collecting empirical dosimetry data and further test estimation models for different animal species and areas with different contamination concentrations and patterns.

## Sammendrag

Måling av ekstern kontaminanteksponering hos vilt er utfordrende, på grunn av mangelen på egnet måleutstyr. Det meste av data om ville dyrs eksponering for kontaminanter er derfor hentet fra simuleringsmodeller, som ERICA Tool. Men, antagelser som brukes og estimater fra modellene blir sjeldent verifisert, på grunn av mangel på empirisk eksponeringsdata. I tillegg vil dosimetrisimuleringene kompliseres den heterogene romlige fordelingen av radionuklider og dyrenes tidsbruk av habitater. Dosimetrimodeller er sentrale komponenter i økologisk risikoanalyse, og det er derfor viktig å verifisere dem.

Vi ville teste 1) om estimater av individuell ekstern dose fra ERICA, basert på gjennomsnittlig kontaminantkonsentrasjon i jord, er konservative, og 2) om estimater forbedres ved å inkludere den heterogene tidsbruken og fordelingen av radionuklider. Vi sammenlignet eksterne  $^{137}\text{Cs}$  doser fra ERICA Tool med empirisk data samlet inn med GPS-koblede dosimetre på tre tamreiner i Jotunheimen, et av områdene i Norge som mottok mest radioaktivt nedfall fra Tsjernobyl-ulykken. Akkumulerte dosemålinger og satellittkoordinater ble innhentet hver time i 5 måneder. GPS-lokasjoner ble brukt til å definere hjemme- og kjerneområde for de tre individene. Radionuklidkonsentrasjon i jord fra radiometriske undersøkelser ble brukt til å finne gjennomsnittskonsentrasjonen av  $^{137}\text{Cs}$  i hele beiteområdet og områdevektet gjennomsnittskonsentrasjoner av  $^{137}\text{Cs}$  i hjemme- og kjerneområder. Doserater ble estimert for både gjennomsnittskonsentrasjon i beiteområder og områdevektet gjennomsnittskonsentrasjon for hjemme- og kjerneområder. Modellerte estimater med gjennomsnittskonsentrasjon for hele beiteområdet var ikke konservative, med en gjennomsnittlig underestimert av ekstern  $^{137}\text{Cs}$  dose hos rein på 70%. Ved å bruke områdevektede gjennomsnittskonsentrasjoner, for å inkludere den romlige og temporale heterogeniteten, ble estimatene noe forbedret, men hadde fortsatt en underestimert på 53% og 46% for arealvektet gjennomsnittskonsentrasjoner i henholdsvis hjemme- og kjerneområde. Dette viser at estimerte doserater med utgangspunkt i data basert på sentrale tendenser i forurensningskonsentrasjoner kan være villedende.

Ved å bruke aktive dosimetre fikk vi informasjon om variasjonen i dose og mulighet til å se på potensialet for å bruke rein til kartlegging av kontaminanter. Dette ble undersøkt ved å se etter korrelasjon mellom eksterne  $^{137}\text{Cs}$  doserater og  $^{137}\text{Cs}$  konsentrasjoner i jord. Resultatene viste en moderat korrelasjon ( $r_s=0.51$  i gjennomsnitt). Det trengs data med høyere doserater og radionuklidkonsentrasjoner for å oppnå mer pålitelige resultater. Videre forskning burde fokusere på innsamling av empirisk dosimetridata og videre testing av estimeringsmodeller for andre dyrearter og områder med ulike konsentrasjoner og fordelinger av forurensende stoffer.

## Table of Content

Acknowledgement.....	I
Abstract .....	II
Sammendrag .....	III
Table of Content.....	IV
List of Figures .....	VI
List of Tables.....	VII
List of Abbreviations.....	VIII
1 Introduction .....	1
2 Background Information .....	5
2.1 Sources of Radiation.....	5
2.1.1 Natural Sources of Radiation - NORM.....	5
2.1.2 Anthropogenic Sources .....	5
2.2 Types of Exposure .....	9
2.3 Wildlife and Radiation.....	9
2.3.1 Measuring Dose Rate Using GPS-Coupled Contaminant Monitors .....	10
2.4 Semi-Domesticated Reindeer as a Study Species.....	10
2.5 Dose Simulation Models .....	11
2.5.1 ERICA Tool .....	12
3 Method .....	14
3.1 Study Area .....	14
3.1.1 Mapping of Radionuclides .....	15
3.2 GPS-Coupled Contaminant Monitors.....	15
3.3 Data Processing .....	16
3.3.1 Home Range Calculations in RStudio.....	16
3.3.2 Data Processing in QGIS.....	17
3.3.3 Data Processing in Excel.....	17
3.3.4 Dose Modelling in ERICA Tool .....	19
3.4 Correcting GPS-Dosimeter Measurements .....	19
3.5 Variation in Dose.....	21
3.6 Reindeer as a “Biotic Contaminant Mapper” .....	21
4 Results and Discussion.....	22
4.1 Utilization Distribution and Concentrations of Radionuclides in Herding Area.....	22
4.1.1 Home Range and Core Area.....	22

4.1.2	Contamination Levels of $^{137}\text{Cs}$ .....	25
4.1.3	Concentration of Potassium, Thorium, and Uranium in Soil.....	27
4.2	GPS-Dosimeter Measurements.....	29
4.2.1	Correction of Dosimeter Measurements .....	29
4.3	ERICA Model Simulations of Dose Rate.....	32
4.4	Information Obtained When Using Active Dosimeters .....	37
4.4.1	Variation in Dose Rate .....	37
4.4.2	Using Reindeer as a “Biotic Contaminant Mapper” .....	42
4.5	Uncertainties .....	45
4.6	Future Research .....	46
5	Conclusions .....	47
	References .....	48
	Appendix .....	53

## List of Figures

Figure 1: Decay scheme of $^{137}\text{Cs}$ .....	6
Figure 2: Maps of $^{137}\text{Cs}$ contamination levels in Norwegian soil (1986/1995) .....	8
Figure 3: Area covered by the aerial survey conducted by NGU .....	14
Figure 4: Reindeer with GPS-dosimeter collar. ....	16
Figure 5: Home ranges, core areas, and GPS locations for all three reindeer.....	23
Figure 6: Contamination levels of $^{137}\text{Cs}$ in herding area.....	25
Figure 7: Distribution of $^{137}\text{Cs}$ levels in herding area, home range and core area .....	26
Figure 8: Concentration of K in herding area.....	28
Figure 9: Concentration of Th in herding area .....	28
Figure 10: Concentration of U in herding area.....	29
Figure 11: Dosimeter measurements and ERICA estimates of external $^{137}\text{Cs}$ dose rate .....	33
Figure 12: Variation and distribution of dose rate throughout the study period .....	39
Figure 13: Variation in dose rate, integrated into 5-day intervals.....	41
Figure 14: Plot of measured external $^{137}\text{Cs}$ dose rates vs levels of $^{137}\text{Cs}$ in soil #37403.....	43
Figure 15: Plot of measured external $^{137}\text{Cs}$ dose rates vs levels of $^{137}\text{Cs}$ in soil #37404.....	44
Figure 16: Plot of measured external $^{137}\text{Cs}$ dose rates vs levels of $^{137}\text{Cs}$ in soil #37405.....	44
Figure 17: Contamination levels of $^{137}\text{Cs}$ in home range and core area #37404.....	56
Figure 18: Contamination levels of $^{137}\text{Cs}$ in home range and core area #37405.....	57

## List of Tables

Table 1: Size of home range and core area for all three reindeer .....	22
Table 2: Percentage of herding area, home ranges and core areas within each of five <sup>137</sup> Cs contamination zones.....	26
Table 3: Area-weighted means for <sup>137</sup> Cs activity levels in home ranges and core areas .....	27
Table 4: Average dose rates of <sup>40</sup> K, cosmic radiation, internal <sup>137</sup> Cs, and corrected GPS- dosimeter measurements for the whole measuring period.....	30
Table 5: Max and min altitude with corresponding cosmic radiation dose rate.....	31
Table 6: Measured external <sup>137</sup> Cs dose rate and dose rate estimates from ERICA Tool.....	33
Table 7: Relative standard deviations for quantified uncertainties.....	45
Table 8: Average altitude in home ranges and core areas.....	55
Table 9: <sup>137</sup> Cs contamination zones with associated proportion of home range and core area#37403.....	55
Table 10: <sup>137</sup> Cs contamination zones with associated proportion of home range and core area #37404.....	55
Table 11: <sup>137</sup> Cs contamination zones with associated proportion of home range and core area #37405.....	56



## List of Abbreviations

a.s.l. – above sea level

CR – cosmic radiation

Cs - caesium

d.w. – dry weight

DCC – dose conversion coefficient

GPS – global positioning system

K - potassium

MSE – mean squared error

NORM – naturally occurring radioactive material

RSD – relative standard deviation

SD – standard deviation

TENORM – technologically enhanced naturally occurring radioactive material

Th – thorium

U - uranium

UD – utilization distribution

w.w. – wet weight

WMS – web map service

## 1 Introduction

Human activities and contaminants, such as radioactive materials, can pose a threat to biodiversity. Ecological risk assessments are essential tools for managing nature and its ecosystems sustainably and protecting the environment from such contaminants (EPA; Suter & Barnhouse, 2007). With nuclear power becoming an important topic as a green alternative to fossil fuel-based energy production, radioecological risk assessments might become increasingly important. For risk assessments to be accurate, we are in need of good, reliable estimation models and methods.

Ecological risk assessments of radioactive contaminants include looking at radiation doses received by organisms in the environment. This can be done either by measuring directly using dosimeters, or by estimating dose using activity concentration in media and dose conversion coefficients (DCCs). Unfortunately, performing real-life measurements is not always feasible, especially for free-ranging animals. Therefore, computer models such as ERICA Tool are often used to simulate wildlife exposure and corresponding radiation dose (Brown et al., 2008). However, modelling dose to wildlife is challenging and associated with relatively large uncertainties, among other things because radionuclides disperse heterogeneously among various habitats in the environment and animals spend varying amounts of time in those habitats. Because of the spatial-temporal variation, using mean contaminant concentration values for a larger area when modelling radiation dose could be inaccurate. Nonetheless, this is a commonly used method when making dose rate estimates (e.g. Beresford et al., 2005; DOE, 2019; EPA, 1996b).

Additionally, dosimetry estimates from models are rarely verified by empirical field measurements on animals. The reason is lack of available empirical exposure data. Obtaining this kind of data is, in fact, a well-known challenge in exposure research and ecological risk assessments in general because of the lack of affordable, durable, easy-to-use contaminant monitors that can be used on free-ranging wildlife (Hinton et al., 2013; NRC, 2012). Even so, verifying model estimates/simulations with real-life measurements is crucial if model results are to be trusted components of ecological risk assessments.

Risk assessments are often conducted in tiers of increasing complexity. The first tier is a scoping assessment. Here, exposure is intentionally maximized (using maximum soil contamination levels) to simulate “worst-case scenarios” and give “conservative” estimations of radiation dose (DOE, 2019). A conservative estimate is typically “non-optimistic” or cautious, being a

“proactive estimate”. Tier 1 calculations result in an estimate considered conservative because they purposely produce an overestimation of radiation dose, numbers expected to be much higher than the actual exposure experienced by biota. If simulated dose from Tier 1 does not exceed dose limits for harmful effects, chances are small that any animal will experience harmful effects of radiation in the area of interest. If estimations from Tier 1 exceed dose limits, one should move on to Tier 2 calculations. Tier 2 is still relatively simple and conservative, but more detailed and customizable than Tier 1. In Tier 2, average soil contamination level is frequently used. Risk evaluators often assume that average soil contamination levels can be used to derive conservative estimates of radiation dose to wildlife, and it is therefore commonly used in estimation models like ERICA Tool (DOE, 2019; EPA, 1996a). Moving on to Tier 3, even more site-specific data is needed, probability is included, and estimates, thus, become more realistic (Brown et al., 2008; DOE, 2019)

Recent advancements in measuring dose to free-ranging animals (Hinton et al., 2015) allowed researchers to test the common risk assessment paradigm that conservative estimates of dose to wildlife can be derived from averaged soil contamination levels (Hinton et al., 2019). The paradigm’s rationale is that animals move randomly across areas of varying contamination levels, and that in the long term they spend similar amounts of time in each. Thus, dose over longer periods can be represented by averaged contaminant concentration in the exposure area (EPA, 1996a). U.S. Environmental Protection Agency’s ecological risk assessment guidance states that “an average concentration term is used in most assessments when the focus is on estimating long-term, chronic exposures” (EPA, 1996b). However, research on wolves (*Canis lupus*) living within the 30 km exclusion zone around Chernobyl discovered that the assumption of conservatism was not valid (Hinton et al., 2019). The use of averaged soil contaminant concentrations under-predicted exposure for some animals, and thus use of averaged contaminant concentrations to predict external exposures was not as conservative as proposed by current risk assessment guidance. If subsequent research supports the conclusions from the Chernobyl wolf study, then risk assessments based on averaged soil contaminant levels might be biased and erroneous, and, as a consequence, lead to wrong management decisions.

Because of heterogeneous distribution of radionuclides in soil, radiation exposure is dependent on animal’s utilization distribution (UD) in its habitat. Hinton et al. (2019) describe utilization distribution as “spatial probability distributions based on the frequency in which animals use portions of the landscape”. A utilization distribution is the probability of finding individuals in a specific area, or in other words, the proportion of time they spend in different areas. Thus,

99% UD tells us in which area there is a 99% chance of finding the animal or where they stay 99% of the time. This is often called the home range of the animal. Likewise, 50% UD tells us in which area there is a 50% chance of finding the animal or where they stay 50% of the time. This is often called the animal's core area, defining areas used most frequently by the animal and often includes resting and foraging sites.

The Chernobyl wolves had large home ranges ( $226\pm 104\text{ km}^2$ ) and small core areas ( $8\pm 7\text{ km}^2$ ) (Hinton et al. 2019). The large size difference in core areas and home ranges of wolves might be a reason the conservative assumption of estimating dose using ERICA Tool and averaged soil contamination levels failed. This casts doubt on whether the wolf study conclusions can be extrapolated to other species and other contaminated areas.

Therefore, we opted to see how the assumption of using averaged soil contamination levels would hold for a species having very different life history characteristics than wolves, namely reindeer (*Rangifer tarandus tarandus*) in Norway. Reindeer are a deer species mainly living in the mountainous areas of Norway (this apply to wild reindeer, reindeer husbandry is practised in other part of the country as well) (Langvatn, 2022). They are nomadic herbivores, following food availability throughout the year. Because of this, their home range and core area are quite extensive. In addition, their core area can consist of several separate areas, as opposed to the Chernobyl wolves' small, concentrated core areas. The data used in this thesis were collected from semi-domesticated reindeer grazing in regions affected by radioactive fallout from the Chernobyl accident (Jotunheimen, west in Innlandet county). Levels of radiocaesium are relatively high, and dosimeter measurements from these animals are of particular interest.

The overall goal for this thesis was to test the conservative method for estimating dose rate in free-ranging wildlife using estimation models, and investigate which variables are important to include to optimize such radiation dose simulations. Dose estimation is an important part of ecological risk assessment processes, which lay the foundation for sustainable and protective management of ecosystems. Thus, we are in need of good, reliable estimation models and methods.

Using the same methods as in the wolf study by Hinton et al. (2019) – tracking animals with GPS-coupled contaminant monitors – and with access to reindeer pastures previously mapped for radionuclides, we tested the following hypotheses:

1. Using mean soil contaminant concentrations in ERICA Tool conservatively estimate individual external dose, and

2. accounting for the spatial-temporal variation of exposure, using area-weighted mean soil contamination levels within each animal's home range (99% UD), gives a more realistic radiation dose estimate.

Additionally, the advanced dosimeter tool (GPS-dosimeters) enabled us to look at variation in dose rate over time for the reindeer. It also allowed us to investigate the possibility of using reindeer as a “biotic contaminant mapper”, to chart areas that are not already mapped and extend the existing radionuclide concentration maps.

## 2 Background Information

### 2.1 Sources of Radiation

Under normal circumstances, most organisms are not exposed to levels of ionizing radiation that would cause any concern of adverse effects. An organism's daily dose can consist of both natural and anthropogenic (man-made) radiation sources. Natural sources are, nevertheless, the most important in the majority of cases. Exceptions can occur in areas with activities like uranium mining and reprocessing of radioactive waste or at the scene of an accident.

#### 2.1.1 Natural Sources of Radiation - NORM

Background radiation comes from natural radiation sources, also called naturally occurring radioactive materials (NORMs). NORMs are minerals and soil in the Earth's crust, and materials in space (*Naturlig forekommende ioniserende stråling*, 2016). Radiation emitted from space is called cosmic radiation and can have its origin from both natural and man-made sources. There are three naturally occurring radioactive decay series; the uranium series, the actinium series, and the thorium series. The uranium series and actinium series originate from  $^{238}\text{U}$  and  $^{235}\text{U}$ , respectively. The thorium series originate from  $^{232}\text{Th}$ . All three end in stable, meaning non-radioactive, lead ( $^{206}\text{Pb}$ ,  $^{207}\text{Pb}$ , and  $^{208}\text{Pb}$ ) (Kónya & Nagy, 2012). There is also the "artificial" neptunium series, no longer natural because the radioactive atoms it consists of are no longer naturally present on Earth (Choppin et al., 2013).

#### 2.1.2 Anthropogenic Sources

In addition to the natural background dose, wildlife organisms can be exposed to ionizing radiation from anthropogenic source. There are two "types" of anthropogenic sources of radiation; those including radionuclides of natural origin, and those including man-made radionuclides. The former is what we call TENORM – technologically enhanced naturally occurring radioactive materials. TENORMs are NORMs that in some way have been handled by humans, which in turn increases exposure to the environment and organisms (EPA, 2008), such as uranium released to the environment from mining sites. An anthropogenic source of radiation where both radionuclide and source are of anthropogenic origin is for example  $^{137}\text{Cs}$  from nuclear weapons and nuclear power production. Medical activities like x-rays and radiotherapy are the most significant contributor to the man-made radiation dose for humans (UNSCEAR, 2010). For biota, the most important anthropogenic sources are nuclear weapon

tests, accidents at nuclear power plants, uranium mining and milling, and discharges from reprocessing plants (Salbu et al., 2015).

The anthropogenic radiation source most relevant for this thesis is nuclear accidents. Accidents leading to radionuclide contamination often happen at nuclear power plants, reprocessing plants, and storage sites. These are all installations holding vast amounts of highly radioactive material, and accidents leading to releases to the environment can cause great damage on cells and genetic materials in organisms, cascading into severe effects on ecosystems. Radionuclides can also spread, transported by wind and water, and substantially affect areas far from accident sites, such as in the Chernobyl accident.

### Caesium-137

Caesium is a reactive alkali metal, present in small amounts in the Earth's crust. Several radioactive isotopes of the element are produced intentionally for medical use, like radiotherapy, and "unintentionally" as a fission product from for example nuclear power production (Kofstad & Pedersen, 2021). One of these radioactive isotopes is  $^{137}\text{Cs}$ , a fission product produced in nuclear weapon detonations and nuclear reactors (EPA, 2021). The decay scheme of  $^{137}\text{Cs}$  is shown in Figure 1. Caesium-137 has a half-life of 30 years (IAEA, 2007); thus, it is a radionuclide of concern for many years if emitted into the environment.

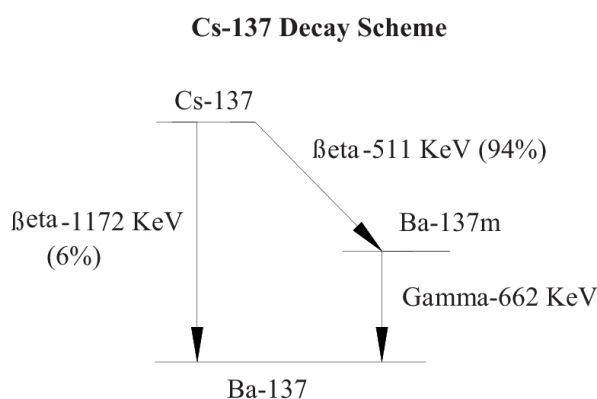


**Figure 1:** Decay scheme of  $^{137}\text{Cs}$ . The majority of  $^{137}\text{Cs}$  (94%) disintegrates to metastable barium ( $^{137m}\text{Ba}$ ) through beta radiation. Then,  $^{137m}\text{Ba}$  disintegrates to stable barium ( $^{137}\text{Ba}$ ) by emitting gamma radiation. When measuring gamma radiation from  $^{137}\text{Cs}$ , it is in fact gamma radiation coming from  $^{137m}\text{Ba}$ . Figure derived from Cafferty, K. G. (2010). *Application of Bayesian and Geostatistical Modeling to the Environmental Monitoring of Cs-137 at the Idaho National Laboratory: University of Idaho.*

Nuclear weapon testing is one of the major sources of  $^{137}\text{Cs}$  in the environment. Tests have been implemented in the atmosphere, on the ground, and under water. They have caused radioactive fallout both globally, regionally, and locally around test sites. Low-yield weapons result in local

tropospheric fallout, while high-yield weapons (thermonuclear weapons) cause contamination of higher atmospheric layers (stratosphere), hence causing global fallout (Ketterer et al., 2004; Aarkrog, 2003). Atmospheric fallout from nuclear weapons has affected many countries worldwide, including Norway. Another significant source of  $^{137}\text{Cs}$  releases to the environment is discharges from reprocessing plants as well as accidents at nuclear power plants (Salbu et al., 2015).

Radionuclides are brought from the atmosphere to the Earth's surface by precipitation (rain and snow) or as dry deposition. Consequently, areas with a high precipitation frequency are often more polluted by radionuclides than more droughty regions. Norway has received  $^{137}\text{Cs}$  fallout from both nuclear weapons testing and power plant accidents. Cs-137 from weapons mainly comes from detonations on the northern hemisphere, where the U.S. and the former Soviet Union executed most of the tests (Biørnstad, 2014). In 1977, the activity concentrations of  $^{137}\text{Cs}$  in Norwegian surface soils ranged between 22 and 525 Bq/kg (d.w.) (Gjelsvik et al., 2014), of which the majority originated from atmospheric testing of nuclear weapons. Fortunately, the amount of radiation-emitting material from weapon test fallout has been relatively low and does not pose a severe risk for Norwegians. Note that the activity concentration is given as Bq/kg dry weight soil. If it was given as Bq/kg wet weight soil the activity concentration would have been lower (525 Bq/kg (d.w.) corresponds to 236 Bq/kg (w.w.) with a soil water content of 55%). Fallout from the nuclear accident at Chernobyl on the other hand has led to consequences for some parts of Norway.

### *The Chernobyl Accident*

When the Chernobyl accident happened on the 26<sup>th</sup> of April 1986, massive amounts of radionuclides were released to the atmosphere. The explosion and following fire in the reactor carried particles as high as 1500 meters up in the air (Strand, 1994). Half of the reactor content was dispersed into the atmosphere and areas local to the plant (Walker et al., 2012). Some of the radionuclides released to the atmosphere were taken by wind and deposited in areas far from Chernobyl Nuclear Power Plant. Because of northwest wind direction at the time of the accident and the following days, some radionuclides were deposited in Norway.

A considerable amount of the radioactive particles precipitated in the middle part of Norway (in the Jotunheimen area) (Figure 2). The fallout consisted mainly of radioactive caesium (30-40%  $^{134}\text{Cs}$  and 60-70%  $^{137}\text{Cs}$ ) (Velle, 2020). Because of the short half-life of  $^{134}\text{Cs}$ , 2.1 years (IAEA, 2004), it is today at negligible levels, while  $^{137}\text{Cs}$ , with a half-life of 30 years, is still present. After the accident, 25 000 Bq/m<sup>2</sup> was measured as average surface soil contamination



level of  $^{137}\text{Cs}$  in Oppland county (now Innlandet county, of which Jotunheimen is a part) (Gjelsvik et al., 2014)<sup>1</sup>. The high contamination levels led to consequences for farmers/herders having animals, mostly reindeer and sheep used for meat production, on pasture in the affected area. Plants take up radioactive nuclides, which are then efficiently taken up in the digestive system of organisms eating the plants (Kofstad & Pedersen, 2021), making products from these animals contaminated. In the following year after the Chernobyl accident, a lot of reindeer meat was discarded due to high levels of  $^{137}\text{Cs}$ . Countermeasures were put into action to avert doses in animals, for example, mixing Prussian blue (a caesium binder) into their fodder (Pedersen, 2021). Still, today countermeasures are implemented, and meat (mainly from reindeer and sheep) is being measured for radioactivity regularly (Miljødirektoratet, 2021).

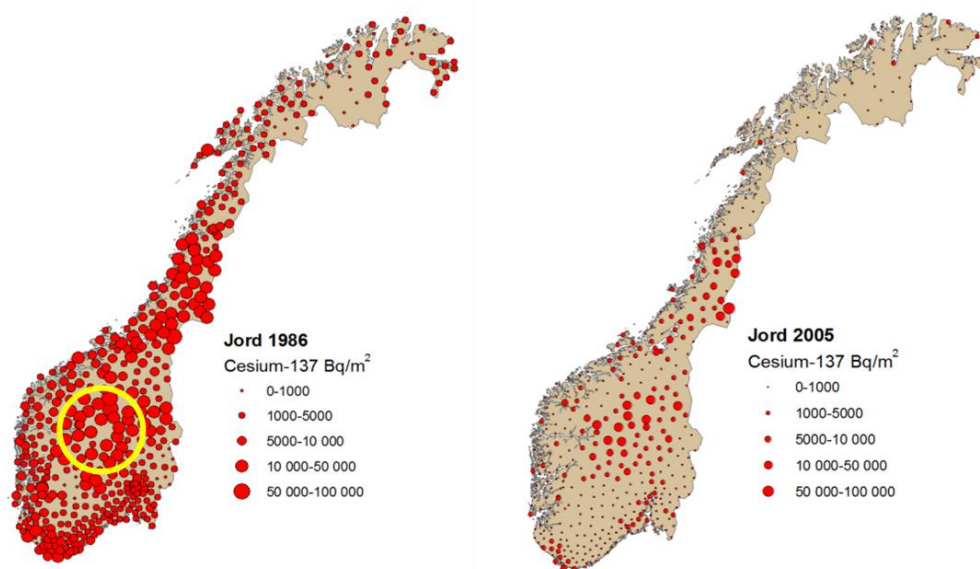


**Figure 2:** Maps of  $^{137}\text{Cs}$  contamination levels ( $\text{Bq}/\text{m}^2$ ) in soil in Norway. The thesis' study area is highlighted with a yellow circle. The map on the left shows contamination levels in 1986, after the Chernobyl accident. Values vary between 440 and 104 000  $\text{Bq}/\text{m}^2$ . The map on the right shows contamination levels in 2005. Values vary between 120 and 69 000  $\text{Bq}/\text{m}^2$ . Figure derived from Gjelsvik, R., Komperød, M., Brittain, J. E., Eikermann, I. M., Gaare, E., Gwynn, J., Holmstrøm, F., Jensen, L. K., Kålås, J. A., Møller, B., et al. (2014). *Radioaktivt cesium i norske landområder og ferskvannssystemer. Resultater fra overvåkning i perioden 1986-2013, 2014:9: Statens strålevern* (Norwegian Radiation Protection Authority).

<sup>1</sup> Different units are used for contaminant levels measured in 1977 ( $\text{Bq}/\text{kg}$  (d.w.)) and 1986/1995 ( $\text{Bq}/\text{m}^2$ ) (Gjelsvik et al., 2014), making it difficult to compare values. Information needed to convert from  $\text{Bq}/\text{m}^2$  to  $\text{Bq}/\text{kg}$ , like soil density and soil water content, is not reported. Using the conversion coefficient calculated based on our data ( $1 \text{ kBq}/\text{m}^2 = 20.8 \text{ Bq}/\text{kg}$  for  $^{137}\text{Cs}$ ), 25 000  $\text{Bq}/\text{m}^2$  equals 520  $\text{Bq}/\text{kg}$ . However, this is not correct, only presented as a basis.

## 2.2 Types of Exposure

Radiation exposure can be categorized into two main types: external and internal exposure. External exposure comes from sources outside of the organism, such as radionuclides in soil, bedrock, water, and the atmosphere. Because of alpha and beta radiation's short range and reduced ability to penetrate an animal's skin, gamma radiation is typically the main radiation type of concern when it comes to external dose rates. External exposure of humans can relatively easily be avoided and reduced, by shielding and simply staying away from areas with high activity concentrations.

Internal exposure comes from radiation sources inside of the organism. Radionuclides can enter an organism's body through several pathways, the most important ones being inhalation and ingestion. They will bioaccumulate in tissue and consequently give rise to internal exposure. Even though it is not well documented, some researchers have even reported biomagnification of some radionuclides in food chains (Harmelin-Vivien et al., 2012; Zhao et al., 2001). Here, alpha and beta emitting radionuclides are of special concern, because of their ability to cause severe damage to cells and DNA. Range is not as important for internal as it is for external exposure, since the source is already inside the body of the organism. The amount of internal radionuclides depends largely on diet. Diets including plants having the ability to accumulate significant amounts of radionuclides, like mushrooms (Gjelsvik et al., 2014), give a greater dose rate from internal exposure. Concerning consumption and human health, internal concentrations of radionuclides affect radioactivity in products coming from animals, like meat and milk.

Even though the two exposure routes must both be considered when calculating overall radiation dose, sometimes, one might want to distinguish between them. In those cases it is important to remember that some measuring methods and instruments register both internal and external radiation, and corrections for one or the other might therefore be needed.

## 2.3 Wildlife and Radiation

Every living creature is exposed to radioactive radiation. Radiation is part of our daily lives, coming from natural and anthropogenic sources. Exposure to radioactivity can be dangerous, and as a potential source of health issues it can have severe consequences for all species. Research on radiation doses and effects on humans have been going on for many decades (e.g. Coggle et al., 1986; Kamiya et al., 2015; Ozasa et al., 2018). There is also research to be found

on animals and other wild organisms (e.g. Krivolutzkii & Pokarzhevskii, 1992; Møller & Mousseau, 2013; Suliman & Alsafi, 2021). Although endpoints are difficult to measure in free-ranging wildlife, reproductive success is thought to be the most sensitive one (IAEA, 1992).

Following nuclear events such as accidents at nuclear power plants or reprocessing plants, radiation dose received by wild organisms can significantly increase. In such situations, research is usually done to obtain information about the condition of individual animals, with speculation on impacts to species and ecosystems. Such accidents also represent an opportunity to investigate possible physiological, behavioural, and genetic effects from chronic exposure to increased radiation (e.g. Anderson et al., 2022; Geras'kin et al., 2008; Mousseau & Møller, 2014). Some research is also done with radiation protection for humans in mind, like monitoring radioactivity in meat from game living in contaminated areas (e.g. Anderson et al., 2022; Cui et al., 2020; Skuterud et al., 2016).

### 2.3.1 Measuring Dose Rate Using GPS-Coupled Contaminant Monitors

It can be hard to measure radiation doses free ranging animals are exposed to. Therefore, estimates from computer models are often used. However, real-life measurements are important to obtain, as they enable us to test and verify these models. To collect such empirical exposure data, animals must be captured – either by using traps or hunting them down – to attach a collar with a dosimeter on them. A GPS can also be included in order to track the animal. Research on wild animals using collars with both an active dosimeter and a GPS unit was first done by (Hinton et al. (2015). The “merging” of these two devices widens the horizon for researchers and makes measuring external radiation exposure easier and more detailed. By coupling external dose received and animal’s location, the data can give a rough presentation of the heterogeneous distribution of radionuclides in the terrain and doses received by the animal at each location.

## 2.4 Semi-Domesticated Reindeer as a Study Species

When using reindeer as a study species, it is often semi-domesticated ones that are being used. These are semi-domesticated reindeer farmed for production of meat and hide, so they are looked after and herded occasionally. Reindeer herders in Northern Norway often move the herd from winter pasture to summer pasture and vice versa twice a year. Further south, the herders keep the animals more or less at the same place all year but herd more actively to keep them inside their restricted pasture area (Ravna & Benjaminsen, 2018). As a result, semi-

domesticated reindeer are out on pasture all year, only gathered once or twice a year during slaughtering. The gathering of animals makes putting on, taking off, and maintaining collars with GPS and dosimeters easier for researchers and most likely less stressful for the animals by taking advantage of them being herded into corrals instead of hunting them down some other time.

So, semi-domesticated reindeer are much wilder than other farm animals, like sheep or cattle, but still partially controlled by humans. A semi-domesticated reindeer will manage all right by itself in the wilderness and can quite easily go from semi-domesticated to wild. On several occasions, semi-domesticated reindeer have been placed in certain areas with the intention that they will “turn wild” and become a new group of wild reindeer (Punsvik et al., 2016). In this way, reindeer can reinhabit areas that, for some reason, have lost their natural wild strain of reindeer. There are no apparent differences between wild and semi-domesticated reindeer, except for their colour (semi-domesticated ones can have different colours and patterns) and their degree of domesticity (Punsvik et al., 2016). Genetically they will differ, but so will groups of wild reindeer. The degree of difference will vary depending on which part of Norway the wild and semi-domesticated reindeer one compares come from. Naturally, wild ones originating from once domesticated animals will share a lot of their genetic material with semi-domesticated reindeer.

For his thesis and the objectives set herein, the animals studied were considered wild reindeer. The ERICA tool is meant to give dose estimates for wild animals, so to be able to compare estimates from ERICA Tool with our data, it must, strictly speaking, come from wild animals. When looking at how reindeer herders keep their animals and the animals’ behaviour, it can be argued that the semi-domesticated reindeer resemble wild ones enough for us to compare results. The herd our data comes from are gathered twice a year, and roam freely for the rest of the year. Naturally, domesticated reindeer will move similarly in the landscape as wild reindeer. They will go to safe places, where access to food and shelter is optimal, and they can keep to themselves. Therefore, the two different “types” of reindeer were compared as if they were the same when it comes to estimating and measuring radiation dose.

## **2.5 Dose Simulation Models**

As it is complicated to do real-life measurements of radiation dose received by organisms, we need other methods to obtain this information. Computer models can be used to simulate

radiation dose and radiological risk to free-ranging animals. As in other risk analyses, the models often use a tiered approach as an easy and cost-efficient method (IAEA, 1999). See the introduction for a more detailed description of this tiered process.

### 2.5.1 ERICA Tool

ERICA (Environment Risk from Ionising Contaminants Assessment and Management) Tool is one such estimation model, estimating radiation risk for biota. It uses dose conversion coefficients (DCCs) to convert activity concentrations in soil/water/air to dose received by organisms (Brown et al., 2008). By entering type of organism, where they live (above, on, or under ground), and conditions concerning radiation (type of radionuclide, activity concentration, soil water content, etc.), the software will give an estimate of the organism's received radiation dose and tell if it is above or below chosen threshold values. Depending on desired accuracy of estimates and how much information one has, one can choose between three different tiers. In Tier 1, much is pre-calculated, and it gives a more general impression of the radiation situation. Tier 2 allows more manual entering and editing, allowing the user to customize the organism and radiation situation to a greater extent. Tier 3 is much like Tier 2 but includes probability.<sup>2</sup>

For ERICA estimates to be reliable, good data on radionuclide concentrations in the media of interest (soil or water) are required. All factors affecting the radionuclides, their activity, and the transfer of radiation must be considered, and their values must be known for the estimates to be precise. Several studies looking at the reliability and accuracy of ERICA Tool estimates have concluded that the estimates are good for some species and habitats but not for others (e.g. Beresford et al., 2008; Hinton et al., 2019; Oughton et al., 2013).

There are many good things about ERICA Tool. It comes in handy when in need of prompt information about dose and radiation risk, e.g., in the case of emergencies where radioactive material has been emitted. It is also helpful for modelling scenarios of potential changes in radionuclide concentrations and composition in an organism's habitat. The user can edit and customize the parameters in Tiers 2 and 3 if more detailed estimates are required. Also, it is free to download and regarded as user-friendly software.

However, one needs to be cautious when using the program. First, it is important to remember that numbers obtained from ERICA are only estimates and do not necessarily represent the true

---

<sup>2</sup> More information about ERICA and how it works can be found at [erica-tool.com](http://erica-tool.com).

situation. In case of a risk assessment, reliable data/estimates are crucial if the assessment is to be trusted. Second, one needs to be extra careful when using Tier 1, where everything is standardized, because the standardized inputs may diverge from reality. For example, finding a standard reference organism with the exact dimensions of the organism of interest can be challenging. Thus, one must put up with the one resembling the most. Third, radionuclides are not evenly distributed, and significant variations in nuclide concentration can occur locally. This heterogeneous distribution, combined with the fact that organisms spend different amounts of time in different areas within their habitat, makes it hard to obtain accurate estimates. To some extent, it can be adjusted for in Tiers 2 and 3, but full correction would be hard, if not impossible, to achieve.

### 3 Method

#### 3.1 Study Area

Data were collected from three reindeer pasturing in the Vågå/Jotunheimen area of Norway (Figure 3) from April through September 2019. The area's altitude varies between 400 and 2400 m, with tree line situated at 900-1000 m (Baranwal et al., 2011). Semi-domesticated reindeer pasture in the area at approximately 1000-1800 m where vegetation is rather sparse and consists of small birch trees, shrubs, heath, moss, and lichens. Above 1500 m, bare rocks are common (Thørring et al., 2019).

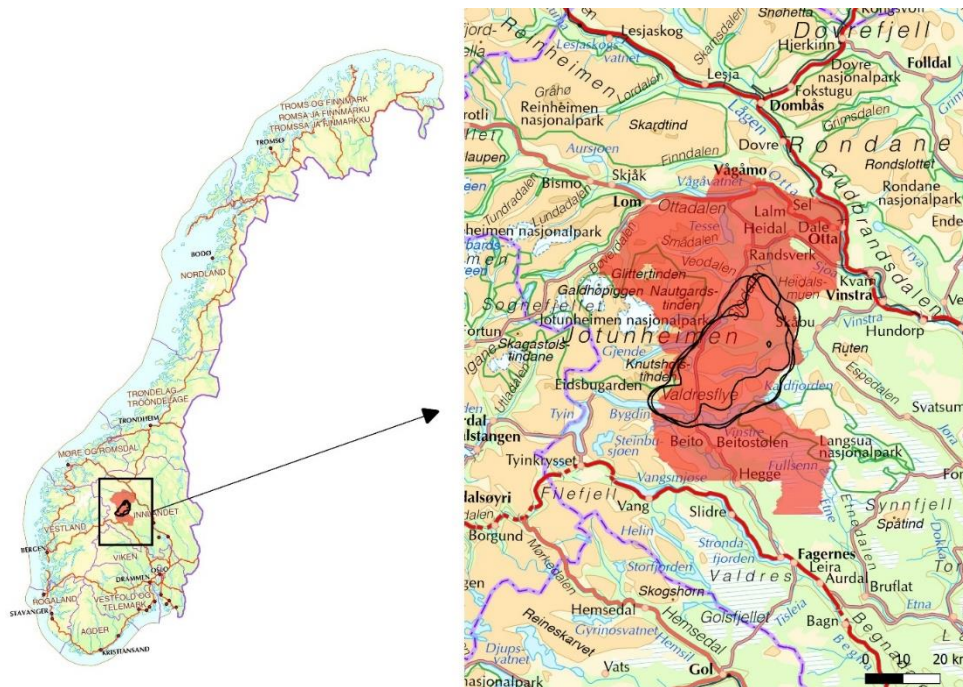


**Figure 3:** Area covered by the aerial survey conducted by NGU for mapping of Cs, K, U and Th (red area). Home ranges for the three reindeer are outlined in black. Map data derived from Statens kartverk. (2007). Toporaster WMS. Available as a web map service (WMS) at: [http://openwms.statkart.no/skwms1/wms.toporaster4\\_](http://openwms.statkart.no/skwms1/wms.toporaster4_)

The Vågå area is part of the region in Norway that received the most radioactive fallout from the Chernobyl accident of April 1986 (Figure 2). After the accident, 25,000 Bq/m<sup>2</sup> was measured as average surface soil contamination level for <sup>137</sup>Cs in Oppland county (now Innlandet county, of which Jotunheimen is a part) (Gjelsvik et al., 2014). The high levels of contamination led to consequences for local herders of reindeer and sheep used for meat production.

Throughout the year, a reindeer's diet changes as they transition between summer- and winter pastures. In summer, they eat fresh grass, herbs, heath, mushrooms, and shrubs (Langvatn, 2022). They gain mass and accumulate fat reserves before winter to survive the harsh climate and periods of limited food. During winter, they eat whatever is available, but the diet consists primarily of lichens (Walker et al., 2012). Lichens efficiently take up nutrients, as well as contaminants, via atmospheric deposition, which is why very high levels of  $^{137}\text{Cs}$  were measured in reindeer meat the first years after the Chernobyl accident (Fremstad, 2019), when radionuclides were deposited directly onto vegetation. Lichens can contain more than 10 times the amount of radiocaesium found in vascular plants (Walker et al., 2012). In later years, mushrooms became an important contributor to  $^{137}\text{Cs}$  uptake by reindeer. Mushrooms are efficient bio-accumulators of Cs from contaminated soil (Gjelsvik et al., 2014) and accumulates  $^{137}\text{Cs}$  to an even greater extent than lichens (Eckl et al., 1986). After the Chernobyl accident, an increased uptake of  $^{137}\text{Cs}$  by mushrooms was documented in several European studies (Heinrich, 1992; Smith et al., 1993; Sugiyama et al., 2008).

### 3.1.1 Mapping of Radionuclides

Levels of radionuclides ( $^{137}\text{Cs}$ ) in the Vågå area were well mapped by the Geological Survey of Norway (NGU), and radioecological research has been ongoing since the Chernobyl accident (e.g. Eikermann et al., 1990; Lønvik & Koksvik, 1990). The total area mapped for radionuclide soil contamination covers 2934 km<sup>2</sup> (red area in Figure 3). An airborne radiometric survey was performed by helicopter in the summer of 2011 (Baranwal et al., 2011) and radionuclide maps were updated in 2020 following extensive ground truthing (Baranwal et al., 2020). In addition to  $^{137}\text{Cs}$  from Chernobyl fallout, the area contains naturally occurring radioactive isotopes ( $^{40}\text{K}$ ,  $^{232}\text{Th}$  and  $^{238}\text{U}$ ) that were mapped as well. All radionuclide maps have a data spacing of ~6 m (Baranwal et al., 2011).

## 3.2 GPS-Coupled Contaminant Monitors

Three semi-domesticated reindeer (#37403, #37404, and #37405), owned by the Vågå herding company (Vågå Tamreinslag), were captured in April 2019 and equipped with GPS-dosimeter collars (Figure 4). Electronic dosimeters (SOR/R) from *Mirion Technologies* were mounted inside the protective housing of the GPS collar from *Vectronic Aerospace GmbH* and coupled electronically (Hinton et al., 2015). Radiation dose was continuously accumulated and transmitted, via satellite, to the researcher each hour, along with the animal's physical location.



Subtraction of dose between time intervals resulted in a dose ( $\mu\text{Gy}$ ) to which the animal was exposed while in the geographical area delineated by the GPS coordinates. Hourly doses were integrated over 24 hours to get a daily dose ( $\mu\text{Gy}/\text{d}$ ). GPS locations were not integrated; they represent the geographical location of the reindeer on an hourly basis. GPS locations and dose rate measurements started on the 17<sup>th</sup> of April and ended on the 19<sup>th</sup> of September 2019. In addition to date, time, geographical coordinates and radiation dose, the data included altitude for each GPS point.



*Figure 4: From a CERAD fieldwork in Valdresfjella in 2019, in connection with the annual herding and slaughter of reindeer in Vågå Tamreinslag. Outlined with a red circle, one of the three female reindeers that were part of this study can be seen with a GPS and electronic dosimeter equipped collar. Photo: O.C. Lind.*

### 3.3 Data Processing

#### 3.3.1 Home Range Calculations in RStudio

GPS and dosimeter data were imported into RStudio (version 2021.09.2 Build 382, R version 4.0.3) and analysed using several packages (adehabitatHR, raster, rgdal, maptools, and rgeos). Approximately 4% of the GPS locations were removed from the analyses because they were outside the area covered by the radionuclide concentrations maps.

Home range, defined as 99% UD, and core area, defined as 50% UD, were quantified for each reindeer using a kernel density estimation model (Fleming & Calabrese, 2017; Silverman, 1986) (package: adehabitatHR). The reference bandwidth (also called smoothing factor) was used,

and grid size was set to 120. The packages raster, rgdal, maptools, and rgeos were used to obtain the size of each reindeer's home range and core area and to convert the data into files suitable for use in QGIS.

### 3.3.2 Data Processing in QGIS

Shapefiles of each reindeer's home range and core area were imported into QGIS (version 3.16.10 "Hannover"). A background map was imported as a WMS (Statens kartverk, 2007). Maps (in raster format) of radionuclide concentrations of K, U and Th in the area were downloaded from the website of Geological Survey of Norway (NGU) (NGU, 2012). An unpublished, updated  $^{137}\text{Cs}$  activity map, as of 2020, was provided to the authors by NGU<sup>3</sup>.

The QGIS function "Join attributed by location" was used to identify GPS points inside each reindeer's home range and core area. Then, "sample raster value" was used to obtain  $^{137}\text{Cs}$ -, K-, U- and Th concentrations at every GPS location, inside both home range and core areas. Cs-137-values for every pixel in the nuclide concentration raster layer (the whole herding area) were also obtained using the "raster pixels to point" function. Finally, "join attributes by locations" was used to obtain  $^{137}\text{Cs}$  concentrations from the raster map for each reindeer's home range and core area.

### 3.3.3 Data Processing in Excel

All information about radionuclide concentrations for the herding area and every GPS location for each reindeer was imported into Excel, together with information about whether locations are inside or outside home range and core area.

#### *Data from Home Range and Core Area*

Because the  $^{137}\text{Cs}$  soil contamination data were mapped in 2016, they were decay-corrected by three years (using Equation 1) to match the GPS-dosimeter measurements taken in 2019.

$$A = A_0 e^{-\lambda t} \quad \text{Equation 1}$$

where  $A$  is soil radioactivity in 2019,  $A_0$  is the soil activity when the map was constructed in 2016,  $\lambda = \ln 2 / \text{half-life of } ^{137}\text{Cs} (30\text{y})$ , and  $t$  is the elapsed time (3 years).

---

<sup>3</sup> The updated version of the  $^{137}\text{Cs}$  contamination level map was sent to us by Vikas Chand Baranwal at NGU.

Furthermore, mapped radionuclide concentrations were published in different units;  $^{137}\text{Cs}$  in  $\text{kBq/m}^2$ , K in %, and U and Th in ppm. The modelling tool ERICA requires soil contamination to be expressed as activity concentration ( $\text{Bq/kg}$  soil). To convert ppm of U and Th to  $\text{Bq/kg}$  (in soil), conversion factors found in the literature were used: 1 ppm =  $\sim 12.44$   $\text{Bq/kg}$  for U (nucleonica.com), and 1 ppm =  $\sim 4.06$   $\text{Bq/kg}$  for Th (Joel et al., 2018). As 0.0117% of the total amount of K present is radioactive potassium ( $^{40}\text{K}$ ), and the activity concentration of  $^{40}\text{K}$  is  $2.617 \times 10^5$ , the factor for converting %K to  $\text{Bq/kg}$  was  $\sim 306$  ( $1\% \approx 306$   $\text{Bq/kg}$ ) (see Appendix A, A.1. for calculations).  $\text{Cs-137}$  was uniformly distributed in the top 3 cm of soil at a soil density of  $1.6 \text{ g/cm}^3$  (Gäfvert et al., 2016), corresponding to a mass depth of  $48 \text{ kg/m}^2$  (Thørring et al., 2019). Thus,  $1 \text{ kBq/m}^2 = 20.8 \text{ Bq/kg}$  (see Appendix A, A.2. for calculations).

After conversion of all concentrations into  $\text{Bq/kg}$  soil, DCCs (dose conversion coefficients) were used to convert radioactivity concentrations into external dose rates ( $\mu\text{Gy/h}$ ). DCCs were obtained from ERICA Tool and were  $9.75\text{E-}5$ ,  $2.13\text{E-}5$ ,  $8.96\text{E-}6$ , and  $3.33\text{E-}6$  for  $^{137}\text{Cs}$ ,  $^{40}\text{K}$ ,  $^{232}\text{Th}$  and  $^{238}\text{U}$ , respectively. Since DCCs obtained from ERICA are based on 100% d.w. soil (0% water content), this needed to be corrected for soil moisture content in the pasture. Soil water content is an average of soil water content values given in Thørring et al. (2019, Appendix C, Table C.2), and was found to be 55%. “Corrected” DCCs were calculated by multiplying the original DCCs with 0.45 (because water content is 55%, the percentage of d.w. soil is 45), and were  $4.39\text{E-}5$ ,  $1.04\text{E-}5$ ,  $4.03\text{E-}6$ , and  $1.5\text{E-}6$  for  $^{137}\text{Cs}$ ,  $^{40}\text{K}$ ,  $^{232}\text{Th}$  and  $^{238}\text{U}$ , respectively.

### *Area-weighted Mean*

Area-weighted mean soil  $^{137}\text{Cs}$  contamination levels in each reindeer’s home range and core area (obtained using data from NGU’s nuclide concentration map, derived in QGIS), were derived using the method described in Hinton et al. (2019). Soil activities were corrected for decay, and divided into contamination zones: 0-20, 20-40, 40-60, 60-80, and  $>80$   $\text{kBq/m}^2$ . The percent within each zone in each home range and core area was calculated, and the median value within each zone was identified (Table 9, Table 10, and Table 11, Appendix B). We obtained an area-weighted mean by summing the percent times median for each zone. Conversion factor ( $\sim 20.8$ ) was used to convert from  $\text{kBq/m}^2$  to  $\text{Bq/kg}$ .

### *Cs-137 Concentration for the Whole Mapping Area*

Mean  $^{137}\text{Cs}$  concentrations were derived for the entire area mapped by NGU’s aerial survey. Numbers were corrected for half-life (3 years, from 2016 to 2019) and converted into  $\text{Bq/kg}$  using the conversion factor ( $\sim 20.8$ ).

### 3.3.4 Dose Modelling in ERICA Tool

ERICA Tool (version 2.0.185), Tier 2, was used to estimate external dose received from  $^{137}\text{Cs}$  soil contamination for reindeer living in the study area. None of the standard reference organisms in the program resembles the physical dimensions of a reindeer, and DCCs are dependent on animal size, so the “new organism” tool in ERICA was used to create a ‘reindeer’. The new reference reindeer weighed 100 kg and measured 1.85 m in length, 0.9 m in height, and 0.5 m in width. These numbers correspond well with the dimensions of a female reindeer given by Langvatn (2022). The “percentage dry weight value” was set to 45% (because water content in soil is 55%). Then, mean  $^{137}\text{Cs}$  concentration for the whole area and area-weighted mean for home range and core area for each reindeer were entered, and external doses were noted. External doses under the same conditions were also obtained for ERICA’s already existing large mammal reference organism. Relative standard deviation concerning mapping of  $^{137}\text{Cs}$  (5%) (O.C. Lind, pers.comm., 2022) was used to calculate the estimates’ standard deviations.

### 3.4 Correcting GPS-Dosimeter Measurements

Our primary goal was to compare external dose as measured with the GPS-dosimeter worn by each reindeer to external dose estimated from soil  $^{137}\text{Cs}$  contamination levels derived with the ERICA Tool. Dose measured by GPS-dosimeters included contributions from  $^{137}\text{Cs}$  within the body of the reindeer, as well as contributions from naturally occurring radionuclides in soil, and cosmic radiation. To obtain external dose received only from  $^{137}\text{Cs}$ , dosimeter measurements were corrected for gamma radiation distribution from other gamma emitting sources present. Here, measurements were corrected for contribution from  $^{40}\text{K}$  in soil, cosmic radiation, and internal  $^{137}\text{Cs}$ .

Cosmic radiation’s contribution to radiation dose depends on where one resides. The higher elevation, the greater the cosmic radiation is. Increase in cosmic radiation as the elevation increases is exponential (0 m a.s.l.=240  $\mu\text{Gy}/\text{year}$ , 1000 m a.s.l.=308  $\mu\text{Gy}/\text{year}$ , 2000 m a.s.l.=471  $\mu\text{Gy}/\text{year}$ , 3000 m a.s.l.=738  $\mu\text{Gy}/\text{year}$  (numbers were found using Equation 2)). In southern/middle part of Norway, reindeer typically live in mountain areas, meaning they receive a substantial radiation dose from cosmic radiation.

Equation 2 was used to calculate cosmic radiation (Cinelli et al., 2017),  $E_1(z)$ , for each GPS point :

$$E_1(z) = E_1(0)[0.21e^{-1.649z} + 0.79e^{0.4528z}] \quad \text{Equation 2}$$

where  $z$  is the altitude in km and  $E_1(0)$  is the annual dose of cosmic radiation at sea level (240  $\mu\text{Gy}$ ). Cosmic radiation was calculated for each GPS point, and the average for each reindeer (average of cosmic radiation for all GPS points) was calculated. Cosmic radiation dose was also found for the highest and lowest altitude registered for each reindeer during the study period.

Whole-body concentrations of  $^{137}\text{Cs}$  for the three reindeer used in this study were determined by analyses of tissue samples by Nikouee (2021). The reindeer were slaughtered in the period 18<sup>th</sup>-20<sup>th</sup> of September 2019, and samples analysed in 2019/2020. Values for the three reindeer were close (905, 956 and 899 Bq/kg w.w.), and thus the average (920  $\pm$ 31 Bq/kg w.w.) was used as the whole-body  $^{137}\text{Cs}$  activity concentration for all three animals. This average was used to calculate internal radiation dose of  $^{137}\text{Cs}$  contributing to the dose registered by the GPS-dosimeters, based on a conversion factor of 0.028 nGy/h per Bq/kg derived by Aramrun et al. (2019) in their study of the same reindeer population. For the  $^{40}\text{K}$  contribution, concentrations of  $^{40}\text{K}$  in soil at each GPS point were obtained from radionuclide concentration maps using QGIS. To convert from percentage of K in soil to Bq/kg a conversion factor of  $\sim$ 306 was used. Then, the corrected DCC was used to convert from Bq/kg to dose rate ( $\mu\text{Gy/d}$ ).

Finally, average cosmic radiation dose rate ( $\mu\text{Gy/d}$ ) for each reindeer, average dose rate ( $\mu\text{Gy/d}$ ) from  $^{40}\text{K}$  for each reindeer, and dose rate ( $\mu\text{Gy/d}$ ) from internal  $^{137}\text{Cs}$  (the same for all three reindeer) were subtracted from average daily radiation dose registered by the GPS-dosimeters for each of the three reindeer. Relative standard deviation (RSD) concerning dosimeter measurements (5%) (O.C. Lind, pers.comm., 2022), internal  $^{137}\text{Cs}$  activity concentration (3%) (Nikouee, 2021), and mapping of K ( $\leq$ 5%) (V.C. Baranwal, pers. Comm., 2022) were combined to get a combined uncertainty for the corrected GPS-dosimeter measurements (see Appendix A for formula used). For mapping of K the maximum value for RSD, 5%, was used.

### 3.5 Variation in Dose

Daily doses were integrated into 5-day doses to look at variation in dose over time for each reindeer. A time series regression analysis was performed on each dataset to create a regression line showing the trend in dose rate over time. Mean squared error (MSE) values were obtained for each regression line.

### 3.6 Reindeer as a “Biotic Contaminant Mapper”

To see if GPS-dosimeters worn by reindeer can be used for contaminant mapping, we compared external dose from  $^{137}\text{Cs}$  quantified by the GPS-dosimeters to  $^{137}\text{Cs}$  activities in soil as mapped by NGU, to look for any correlation. Intervals of 24 hours with associated daily dose ( $\mu\text{Gy/d}$ ) registered on GPS-dosimeters were identified. Cosmic radiation, daily dose from  $^{40}\text{K}$  in soil, and daily dose from internal  $^{137}\text{Cs}$  were calculated for the same 24 hours intervals. These were subtracted from the GPS-dosimeter daily dose, to obtain external daily dose from  $^{137}\text{Cs}$  only. Then, contamination levels of  $^{137}\text{Cs}$  in soil for each interval were obtained by calculating the mean  $^{137}\text{Cs}$  activities ( $\text{kBq/m}^2$ ) for GPS locations within those 24 hours. Lastly, mean soil  $^{137}\text{Cs}$  activity levels for each 24-hour interval were plotted against the corresponding external  $^{137}\text{Cs}$  daily dose ( $\mu\text{Gy/d}$ ). Spearman correlation test was run to obtain a  $r_s$  value. This was done for all three reindeer.

## 4 Results and Discussion

### 4.1 Utilization Distribution and Concentrations of Radionuclides in Herding Area

#### 4.1.1 Home Range and Core Area

Home ranges and core areas are presented in Table 1 and Figure 5. The mean ( $\pm$ SD) area of home ranges for the three reindeer was  $833\pm 146$  km<sup>2</sup>. The smallest range was 665 km<sup>2</sup> (#37403) and the largest was 932 km<sup>2</sup> (#37405). Home range constituted on average 28% of the herding area. The mean ( $\pm$ SD) core area for the three reindeer was  $160\pm 71$  km<sup>2</sup>. The smallest core area was 83 km<sup>2</sup> (#37403) and the largest was 221 km<sup>2</sup> (#37404). Core areas constituted 12%, 25%, and 19% of the home range for #37403, #37404, and #37405, respectively. On average core areas constituted 19% of their home range. For #37404 and #37405 core area consists of several separate areas (see Figure 5).

**Table 1:** Size of home range and core area (km<sup>2</sup>) for all three reindeer, calculated using GPS locations for each individual and the kernel density estimation model (in RStuido). Home ranges' percentage of herding area and core areas' percentage of home range is given. Averages ( $\pm$ SD) are also presented.

	<b>37403</b>	<b>37404</b>	<b>37405</b>	<b>Average <math>\pm</math> SD</b>
<b>Home range (km<sup>2</sup>)</b>	665	903	932	833 $\pm$ 146
<b>% of herding area</b>	22.7 %	30.8 %	31.8 %	28.4 $\pm$ 5.0%
<b>Core area (km<sup>2</sup>)</b>	83	221	176	160 $\pm$ 71
<b>% of home range</b>	12.4 %	24.5 %	18.8 %	18.6 $\pm$ 8.3%

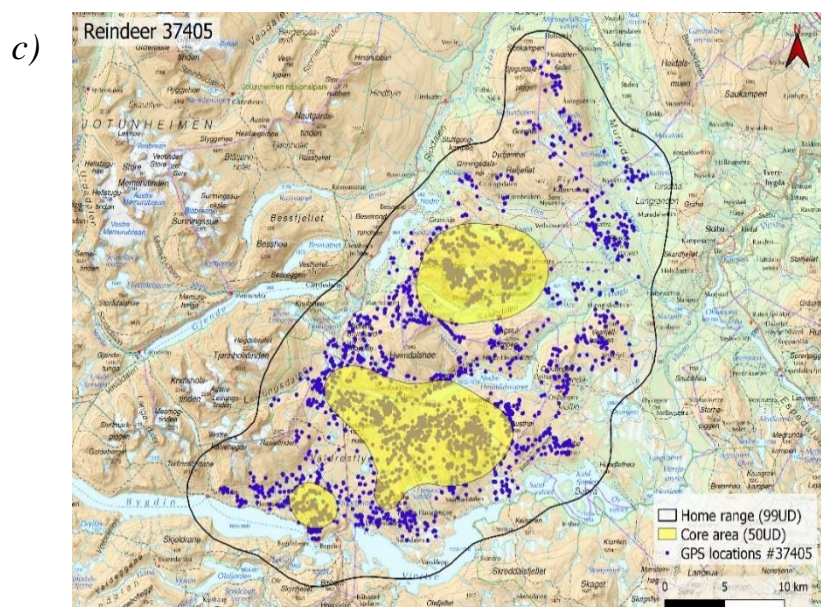
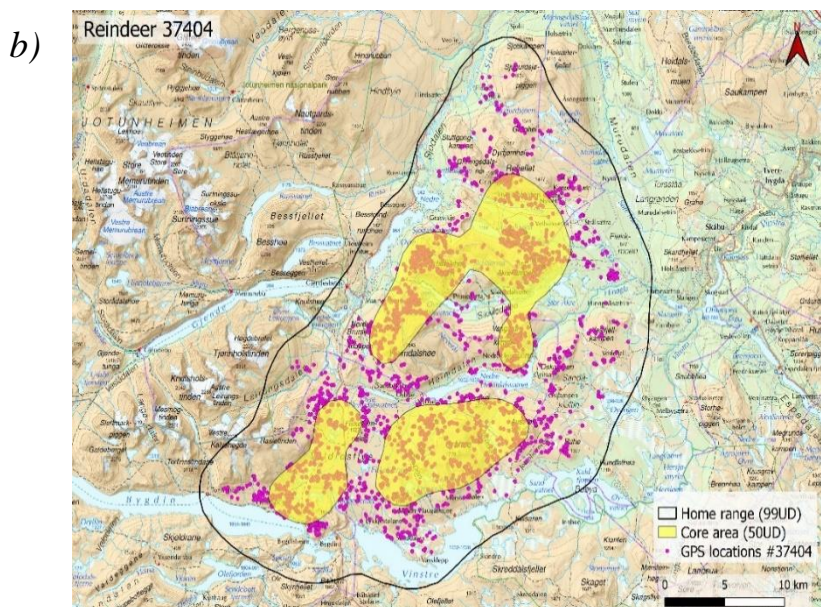
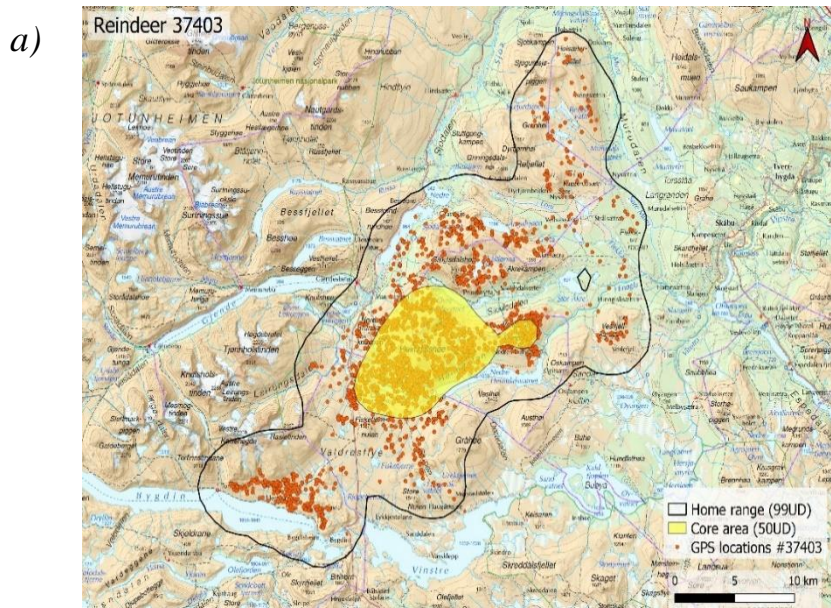


**Figure 5:** Home range (outlined in black), core area (yellow area(s)), and GPS locations for reindeer 37403 (a), 37404 (b), and 37405 (c). Map data derived from Statens kartverk. (2007). Toporaster WMS. Available as a web map service (WMS) at: <http://openwms.statkart.no/skwms1/wms.toporaster4>.



All GPS locations were included in the 99% utilization distribution zones for each reindeer (Figure 5). This is realistic, since 99% UD (the home range) is the area we expect to find the reindeer 99% of the time. Home ranges were neither too under- nor oversmoothed. Therefore, using the kernel density estimation model was a reasonable choice. There is some distance between home range borders and the GPS points closest to the border. This is because the model includes an uncertainty area around each GPS point. How far/close the distance is, depends on the smoothing factor, which in this case is set to a reasonable value (the reference band width). Figure 5 also shows that core areas, 50% UD, were derived from areas with the highest density of GPS points.

Reindeer are nomadic animals, following food availability throughout the year. As a result, their home range can be quite large. This is also seen in other large herbivores, like the moose (*Alces Alces*), and is largely a consequence of the spatiotemporal changes in quality and quantity of food resources (van Beest et al., 2011). Usually, herbivores have a “built-in routine” and go to the same grazing areas each year. But there are factors affecting their choice of pasture, hence affecting size and location of their home range, among other things pasture quality, snow/ice cover and weather. Periods of thick snow cover or severe winter temperatures causing ice to cover vegetation can force reindeer to move longer distances to find food, expanding their home range. Also, human activity can change a reindeer’s movement pattern, both in wild and semi-domesticated populations (Skarin & Åhman, 2014; Vistnes & Nellemann, 2007). Here, some of the GPS locations were removed (those located outside of the radionuclide maps/herding area), so our calculated home range is somewhat smaller than the “true” home range. However, locations removed made up only 1-4% of the total number of GPS locations. Thus, home ranges presented here are still representative of the (semi-domesticated) reindeer’s home range and can be used for our purpose.

The reindeer’s core areas were relatively large, on average covering almost 20% of their home range. For #37404 and #37405 core areas were also “patchy”, consisting of several separate areas. Because of changes in food availability through the seasons, reindeer cannot stay in the same place for long periods. Neither are they dependent on a specific breeding site for a longer period of time. Therefore, they will not have a distinct, concentrated, small core area, as was observed for Chernobyl wolves (mean core area of 8 km<sup>2</sup> was just 3% of mean home range (Hinton et al., 2019) and brown bears (Pop et al., 2018). Thus, reindeer, with life history characteristics different from wolves, proved to be a good species to test the conclusions of Hinton et al. (2019).

#### 4.1.2 Contamination Levels of $^{137}\text{Cs}$

Soil  $^{137}\text{Cs}$  activities in the overall herding area are presented in Figure 6, and divided into five different contamination zones (0-20, 20-40, 40-60, 60-80, >80  $\text{kBq/m}^2$ ) within Table 2. Table 2 and Figure 7 presents percentage of herding area, home ranges and core areas contaminated by the different groupings of  $^{137}\text{Cs}$  soil contamination. All  $^{137}\text{Cs}$  contamination level values were associated with 5% uncertainty. As of 2019, 54% of the herding area had a soil  $^{137}\text{Cs}$  contamination level less than 20  $\text{kBq/m}^2$ , whereas contaminant levels >80  $\text{kBq/m}^2$  covered ~3  $\text{km}^2$  (0.1%), with a maximum concentration of 100  $\text{kBq/m}^2$  (based on radionuclide maps from NGU (Baranwal et al., 2020), half-life corrected for 3 years).

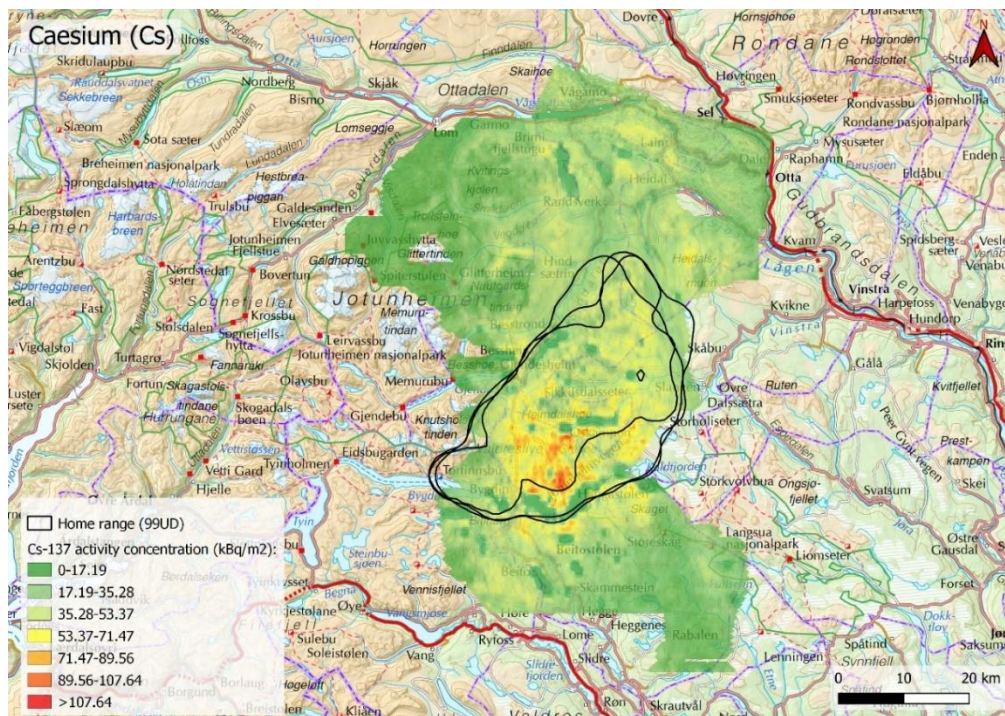


**Figure 6:** Contamination levels of caesium,  $^{137}\text{Cs}$ , in the herding area (in  $\text{kBq/m}^2$ ) as of 2016. Home ranges of the reindeer are outlined in black. Contamination levels are not decay corrected but do still represent the distribution of  $^{137}\text{Cs}$  in the area. Mapdata derived from: 1) Statens kartverk. (2007). Toporaster WMS. Available as a web map service (WMS) at: <http://openwms.statkart.no/skwms1/wms.toporaster4>, 2) NGU (Geological Survey of Norway). (2020). Unpublished.

**Table 2:** Percentage of herding area, home ranges and core areas within each of the five soil radioactivity contamination zones (0-20, 20-40, 40-60, 60-80, >80 kBq/m<sup>2</sup>). Data is derived from maps of <sup>137</sup>Cs concentration in soil from NGU (Geological survey of Norway) using a geographic information system software (QGIS).

kBq/m <sup>2</sup>	Herding area	Home range			Core area		
		37403	37404	37405	37403	37404	37405
0-20	54.4 %	19.1 %	22.0 %	21.7 %	16.5 %	10.4 %	12.4 %
20-40	38.4 %	57.0 %	53.6 %	54.2 %	44.2 %	56.8 %	47.5 %
40-60	6.2 %	19.9 %	20.6 %	20.3 %	37.0 %	24.5 %	30.0 %
60-80	0.9 %	3.5 %	3.4 %	3.3 %	2.3 %	7.6 %	9.7 %
>80	0.1 %	0.5 %	0.4 %	0.4 %	0.1 %	0.7 %	0.5 %

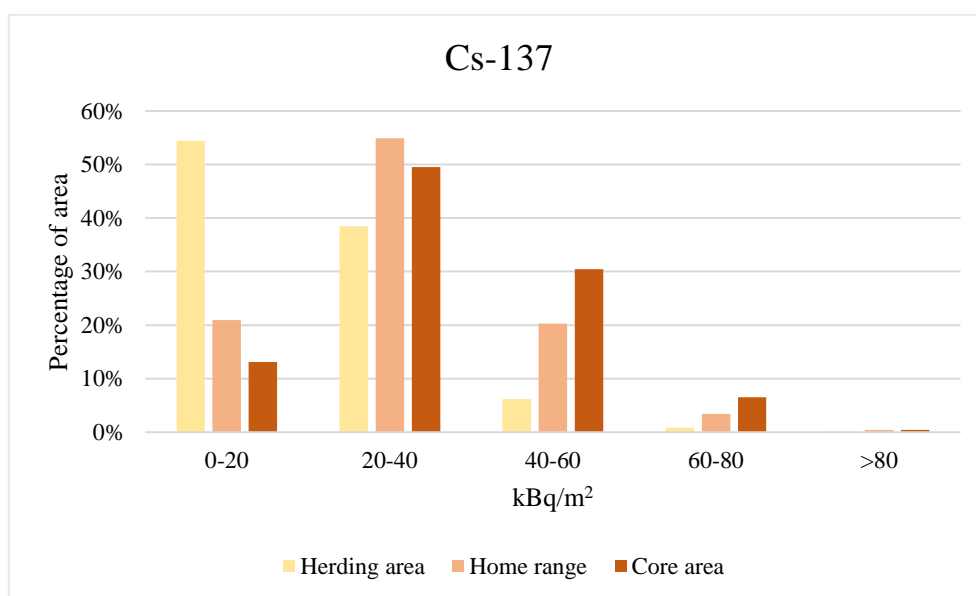


**Figure 7:** The distribution of <sup>137</sup>Cs contamination levels (in kBq/m<sup>2</sup>) in herding area, home range and core area in percentage. Note that for home range and core area the average for the three reindeer is used.

Mean soil <sup>137</sup>Cs activity in the overall herding area was 19.9 kBq/m<sup>2</sup> (414 Bq/kg). Maximum contamination level in herding area was 107.6 kBq/m<sup>2</sup> (2238 Bq/kg). Area-weighted mean soil <sup>137</sup>Cs activity within each reindeer's home ranges was greater than for the overall herding area, 31.6, 31.0, and 30.8 kBq/m<sup>2</sup> for #37403, #37404, and #37405, respectively (Table 3).

**Table 3:** Area-weighted means for  $^{137}\text{Cs}$  activity concentration in home range and core area for all three reindeer, in both  $\text{kBq/m}^2$  and  $\text{Bq/kg}$  soil. To obtain area-weighted means the percent within each contamination zone (0-20, 20-40, 40-60, 60-80, >80  $\text{kBq/m}^2$ ) in each home range and core area was calculated. Then, the percent times median for each zone were summed up for each home range and core area.

	<b>37403</b>		<b>37404</b>		<b>37405</b>	
<b>Area-weighted mean:</b>	$\text{kBq/m}^2$	$\text{Bq/kg}$	$\text{kBq/m}^2$	$\text{Bq/kg}$	$\text{kBq/m}^2$	$\text{Bq/kg}$
<b>Home range</b>	31.6	659	31.0	646	30.8	642
<b>Core area</b>	34.7	723	36.2	754	37.6	784

Area-weighted means (31.6, 31.0, and 30.8  $\text{kBq/m}^2$  for #37403, #37404, and #37405, respectively) were much higher, by a factor of 0.56 on average, than the grand mean for the whole herding area (19.9  $\text{kBq/m}^2$ ). This indicates that the reindeer spent more time in areas with higher  $^{137}\text{Cs}$  activity concentrations, probably because these were areas with sufficient food supply. More than 50% of the whole herding area has an activity of  $\leq 20 \text{ kBq/m}^2$  and only 6.2% has an activity of 40-60  $\text{kBq/m}^2$  (Table 2, Figure 7). In contrast, home ranges consisted of 19-22%  $\leq 20 \text{ kBq/m}^2$  and ~20% 40-60  $\text{kBq/m}^2$ . Area-weighted means for core areas were even higher than for the home ranges (Table 3), which indicates that the reindeer spent more time in the higher contaminated areas relative to lower contaminated areas of their home range. It is pronounced that core areas contained a higher percentage of area in the 40-60 and 60-80  $\text{kBq/m}^2$  contamination zones than occurred in the respective home ranges (Table 2, Figure 7).

#### 4.1.3 Concentration of Potassium, Thorium, and Uranium in Soil

Average soil  $^{40}\text{K}$  activity concentration in the entire herding area (Figure 8) was 373.6  $\text{Bq/kg}$ . Within reindeer home ranges, average activity concentrations were 474.4, 408.8, and 421.1  $\text{Bq/kg}$  for #37403, #37404, and #37405, respectively. Maximum  $^{40}\text{K}$  activity concentration value registered was 1052  $\text{Bq/kg}$  (#37405), and minimum value was 36.4  $\text{Bq/kg}$  (#37404).

In comparison, Th and U activity concentrations were two orders of magnitude lower. Average soil Th ( $^{232}\text{Th}$ ) and U ( $^{238}\text{U}$ ) activity concentrations in the herding area (Figure 9 and Figure 10, respectively) were 6.8 and 6.0  $\text{Bq/kg}$ , respectively. Average activity concentrations for all three home ranges were 4.2  $\text{Bq/kg}$  for Th and 4.6  $\text{Bq/kg}$  for U.

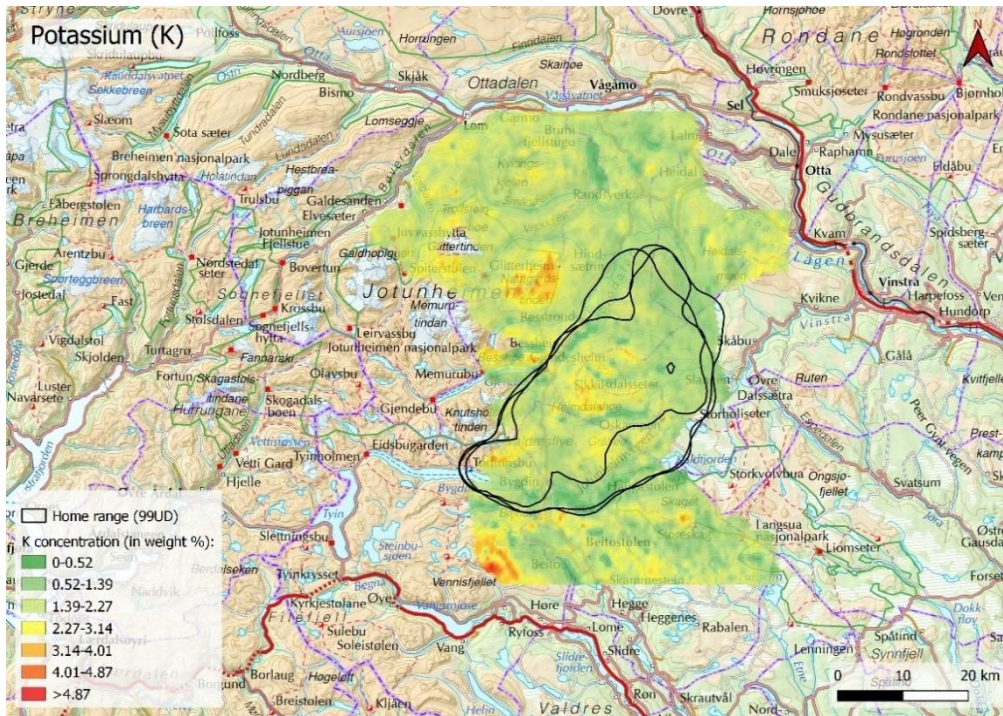


**Figure 8:** Concentration of potassium (K) in the herding area (in weight %). Home ranges of the reindeer are outlined in black. Map data derived from Statens kartverk. (2007). Toporaster WMS. Available as a web map service (WMS) at: <http://openwms.statkart.no/skwm1/wms.toporaster4>, 2) NGU (Geological Survey of Norway). (2012). R\_K\_mic\_f. Available at: <https://geo.ngu.no/geoscienceportalopen/Results?minLong=8.29&maxLong=9.99&minLat=61.20&maxLat=62.31>.

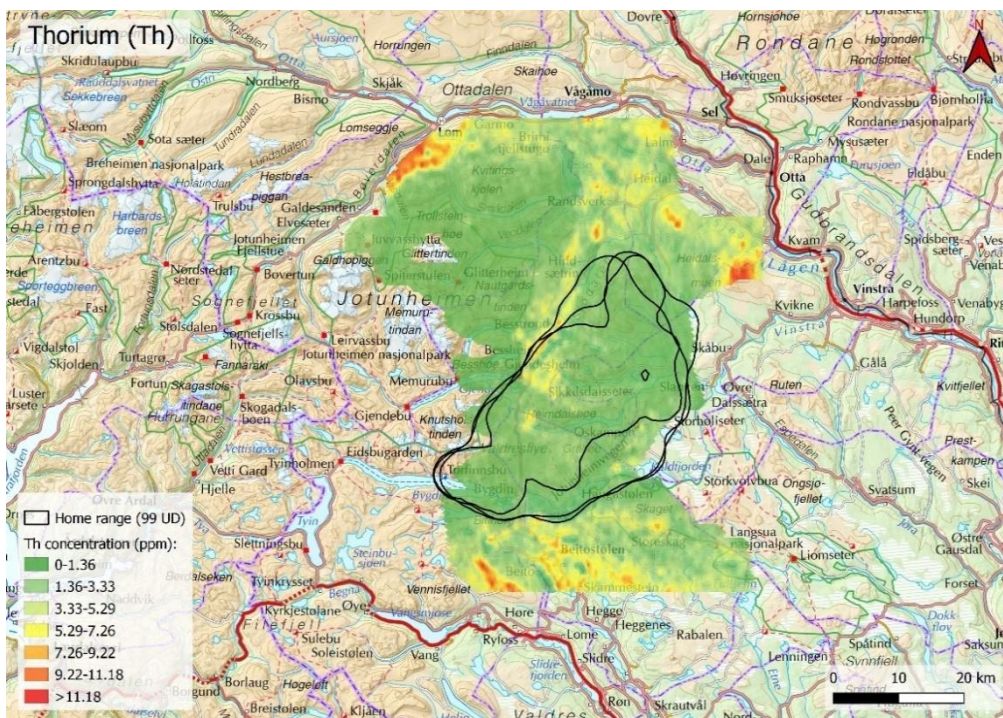


**Figure 9:** Concentration of thorium (Th) in the herding area (in ppm). Home ranges of the reindeer are outlined in black. Map data derived from Statens kartverk. (2007). Toporaster WMS. Available as a web map service (WMS) at: <http://openwms.statkart.no/skwm1/wms.toporaster4>, 2) NGU (Geological Survey of Norway). (2012). R\_Th\_mic\_f. Available at: <https://geo.ngu.no/geoscienceportalopen/Results?minLong=8.29&maxLong=9.99&minLat=61.20&maxLat=62.31>.

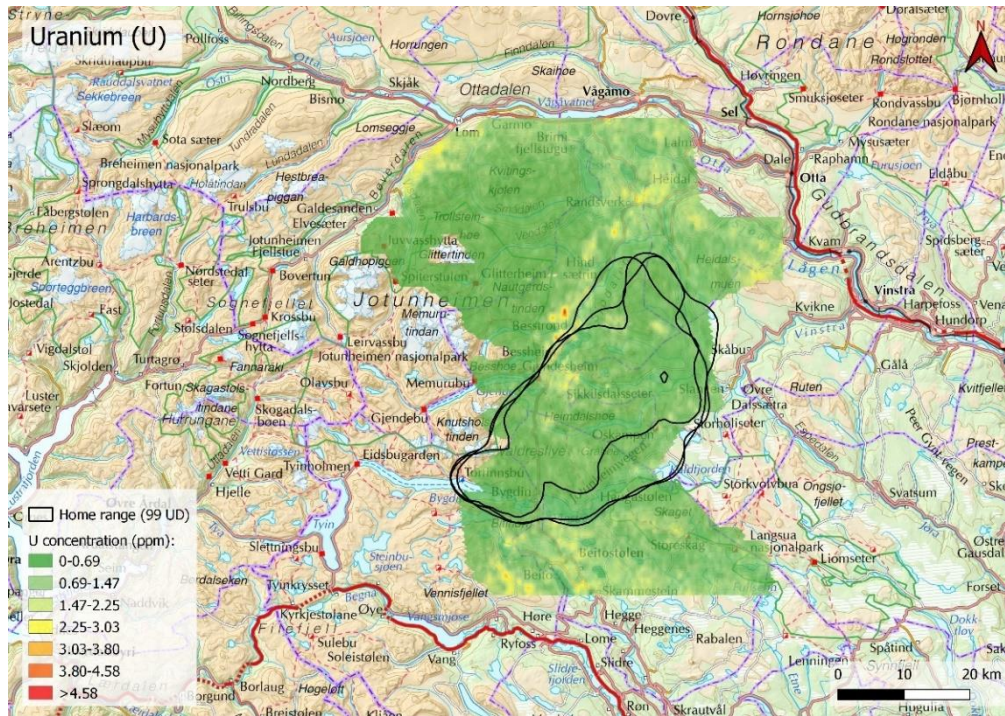


**Figure 10:** Concentration of uranium (U) in the herding area (in ppm). Home ranges of the reindeer are outlined in black. Map data derived from Statens kartverk. (2007). Toporaster WMS. Available as a web map service (WMS) at: [http://openwms.statkart.no/skwms1/wms.toporaster4\\_2](http://openwms.statkart.no/skwms1/wms.toporaster4_2), 2) NGU (Geological Survey of Norway). (2012). *R\_U\_mic\_f*. Available at: <https://geo.ngu.no/geoscienceportalopen/Results?minLong=8.29&maxLong=9.99&minLat=61.20&maxLat=62.31>.

## 4.2 GPS-Dosimeter Measurements

Measurements from GPS-dosimeters were acquired at hourly intervals. However, hourly doses were small relative to radioactivity detection levels of the dosimeters, and thus did not necessarily register as changes in dose rates for every hour. Therefore, hourly doses were integrated into daily doses. Uncorrected (see below) typical external doses measured by the GPS-dosimeters were  $\sim 3 \mu\text{Gy/d}$ , with daily doses ranging from 1-5  $\mu\text{Gy}$ . Doses could also have been integrated into weekly or monthly values, but then a lot of information about the variance in dose rates would be lost.

### 4.2.1 Correction of Dosimeter Measurements

Contributions from cosmic radiation, internal  $^{137}\text{Cs}$ , and  $^{40}\text{K}$  present in soil were subtracted from mean total daily dose rate ( $\mu\text{Gy/d}$ ) measured by the GPS-dosimeter worn on each reindeer (Table 4). After correcting for these three, mean external  $^{137}\text{Cs}$  dose rates ( $\pm\text{SD}$ ) measured by GPS-dosimeters were  $1.5\pm 0.2$ ,  $1.4\pm 0.2$ , and  $1.5\pm 0.2 \mu\text{Gy/d}$  for reindeer #37403, #37404, and #37405, respectively (Table 4).

**Table 4:** Average dose rates ( $\mu\text{Gy}/\text{d}\pm\text{SD}$ ) of  $^{40}\text{K}$ , cosmic radiation, internal  $^{137}\text{Cs}$ , and corrected GPS-dosimeter measurements for each of the three reindeer for the whole measuring period. Dose rates from  $^{40}\text{K}$  (with an uncertainty of 5%) are derived from maps of  $^{40}\text{K}$  concentration in soil from NGU (Geological survey of Norway) and GPS locations of each reindeer, using a geographic information system software (QGIS). Cosmic radiation is calculated using altitude registered by GPSs. Dose rate from internal  $^{137}\text{Cs}$  (with an uncertainty of 3%) is obtained from measurements of gamma radiation in tissue samples, derived from Nikouee, K. (2021). Biodistribution of radionuclides in reindeer from Vågå, Norway. Master thesis: Norwegian University of Life Sciences.

	Dose rate ( $\mu\text{Gy}/\text{d}$ )		
	37403	37404	37405
<b><math>^{40}\text{K}</math></b>	0.118 $\pm$ 0.006	0.102 $\pm$ 0.005	0.105 $\pm$ 0.006
<b>Cosmic radiation</b>	0.98	0.95	0.96
<b>Internal <math>^{137}\text{Cs}</math></b>	0.62 $\pm$ 0.02	0.62 $\pm$ 0.02	0.62 $\pm$ 0.02
<b>Corrected GPS-dosimeter measurement</b>	1.5 $\pm$ 0.2	1.4 $\pm$ 0.2	1.5 $\pm$ 0.2

Because of the long half-life of  $^{40}\text{K}$ ,  $1.25 \times 10^9$  years (IAEA, 2017),  $^{40}\text{K}$  soil concentrations were not decay-corrected as they were for  $^{137}\text{Cs}$ . There were also other gamma sources present in soil (i.e. Th and U) that were mapped in the same way as  $^{137}\text{Cs}$  and K (Baranwal et al., 2011). Due to their low activity concentrations and mode of radioactive emission the daily doses from Th and U were on average  $4.07 \times 10^{-4}$  and  $1.65 \times 10^{-4}$   $\mu\text{Gy}$ , respectively. Their contribution to doses recorded by GPS-dosimeters were insignificant and not taken into consideration here.

### *Cosmic Radiation*

Cosmic radiation varied depending on altitude of the reindeer's location. Average dose rate from cosmic radiation was  $\sim 1$   $\mu\text{Gy}/\text{d}$  (Table 5). On average there was a difference of 0.4  $\mu\text{Gy}/\text{d}$  between max and min dose rates from cosmic radiation, over the length of the study, for the three reindeer (Table 5), which is a lot considering that the minimum value was  $\sim 0.8$   $\mu\text{Gy}/\text{d}$ . Aramrun et al. (2019) conducted a dose rate study on the same reindeer herd and the same area as in our study, however, they used passive dosimeters that did not permit daily delineation of dose rates. Our average cosmic radiation values corresponded well with values from Aramrun et al. (2019) ( $297 \pm 40$   $\mu\text{Gy}/11$  months, corresponding to  $0.89 \pm 0.12$   $\mu\text{Gy}/\text{d}$ ). Following  $^{137}\text{Cs}$ , cosmic radiation was the major contributor of dose to our reindeer.

**Table 5:** Maximum and minimum altitude (m) of the reindeer during the measuring period, with corresponding dose rates ( $\mu\text{Gy/d}$ ) from cosmic radiation (CR). Average altitude and corresponding cosmic radiation are also presented for each reindeer. Dose rates calculations are based on altitude registered by the GPSs

	37403		37404		37405	
	Altitude (m)	CR ( $\mu\text{Gy/d}$ )	Altitude (m)	CR ( $\mu\text{Gy/d}$ )	Altitude (m)	CR ( $\mu\text{Gy/d}$ )
<b>Max</b>	1846	1.2	1771	1.17	1764	1.16
<b>Min</b>	782	0.78	819	0.79	744	0.77
<b>Average</b>	1359	0.98	1293	0.95	1311	0.96

### *Internal Dose from Ingestion of $^{137}\text{Cs}$ Contaminated Food*

Radionuclides in food and water can be consumed by organisms and result in an internal dose. Cs-137 is taken up from soil by plant roots and transported up to the plant parts above ground (Zhu & Smolders, 2000). When these plant parts are ingested,  $^{137}\text{Cs}$  is absorbed in the digestive system of the animal (Kofstad & Pedersen, 2021). In this way organisms take up radionuclides and other harmful contaminants present in the environment. Internal contamination levels (whole-body concentration) in our reindeer were obtained from measurements of  $^{137}\text{Cs}$  in a number of tissues after each animal was slaughtered (Nikouee, 2021). Activity concentrations of  $^{137}\text{Cs}$  in tissues were similar among the three animals (0.905, 0.956, and 0.899 Bq/kg), so an average value was used ( $920 \pm 31$  Bq/kg w.w.) to correct the GPS-dosimeter data for contributions from internal contamination. The average tissue activity concentration of  $^{137}\text{Cs}$  resulted in a dose rate of  $0.62 \pm 0.02$   $\mu\text{Gy/d}$  (based on conversion factor in Aramrun et al. (2019)) contributing to the external dose measured by the GPS-dosimeters. Internal dose to reindeer is slightly higher than Aramrun et al. (2019) reported ( $160 \pm 27$   $\mu\text{Gy}/11$  months, corresponding to  $0.48 \pm 0.08$   $\mu\text{Gy/d}$ ), but can be explained by individual difference between animals and time of the study. Age of the reindeer, time of year the measurements were taken, differences in plants' uptake of  $^{137}\text{Cs}$  due to weather, small differences in diet preferences, etc., are all factors that will affect internal  $^{137}\text{Cs}$  activity concentration measured between different studies. Also, Nikouee (2021) measured internal  $^{137}\text{Cs}$  activity concentrations in the laboratory from tissue samples taken after the animals were slaughtered, while Aramrun et al. (2019) used live-monitoring methods which typically have a lower precision because of the brief amount of time available to monitor a live animal under physical restraint.



The biodistribution of radiocaesium in an organism is debated (Sato et al., 2015), but according to the International Commission on Radiological Protection (ICRP) it is distributed more or less evenly throughout the body (ICRP, 1979). Based on this we can compare our values of whole body activity concentration of  $^{137}\text{Cs}$  ( $920\pm 31$  Bq/kg w.w.) with numbers on  $^{137}\text{Cs}$  activity concentration in muscular tissue in reindeer from a study by Macdonald et al. (2007). Reindeer and caribou in northern Canada, Alaska, and Greenland were studied and activity concentration up to  $\sim 1000$  Bq/kg muscle tissue (w.w.) were reported in the late 1980s. However, the majority of herds had  $^{137}\text{Cs}$  activity concentrations far below 600 Bq/kg, and only a small part of it is reported to originate from Chernobyl (Macdonald et al., 2007). Situated far from Chernobyl, Canada and neighbouring areas did not receive the same amount of radioactive fallout as Norway and other Scandinavian countries. So, the observations made in this comparison were as expected.

### **4.3 ERICA Model Simulations of Dose Rate**

All dose rate estimates from ERICA Tool are presented in Table 6 and Figure 11. Using mean soil  $^{137}\text{Cs}$  concentration in the herding area, ERICA calculations resulted in a dose rate estimate of  $0.44$   $\mu\text{Gy/d}$  for reindeer. This is the same for all three reindeer since herding area, thereby also the grand mean, is the same for all of them. Area-weighted mean soil  $^{137}\text{Cs}$  concentrations within home ranges and core areas resulted in ERICA dose rate estimates of  $\sim 0.7$   $\mu\text{Gy/d}$  and  $\sim 0.8$   $\mu\text{Gy/d}$ , respectively, for all three animals. Doing the exact same with ERICA's pre-programmed generic large mammal (a deer of 245 kg mass) as the target organism for the assessment, dose rates were somewhat lower than for reindeer (100 kg mass, see Table 6).

**Table 6:** Average external daily doses of  $^{137}\text{Cs}$  measured by the dosimeters (corrected for contribution from cosmic radiation, internal  $^{137}\text{Cs}$  and  $^{40}\text{K}$ ) and dose rate estimates from ERICA Tool for both the “new-made” reindeer and ERICA’s generic large mammal. Estimates are based on concentration level data from aerial mapping of the herding area. Estimates using mean soil concentration for the whole herding area are considered conservative estimates. The aerial mapping of  $^{137}\text{Cs}$  has an uncertainty of 5%. Average external  $^{137}\text{Cs}$  dose rates from GPS-dosimeters have a combined uncertainty of ~14%.

		External $^{137}\text{Cs}$ dose rate ( $\mu\text{Gy/d} \pm \text{SD}$ )		
		37403	37404	37405
Measurements from GPS-dosimeters	Average daily dose	$1.5 \pm 0.2$	$1.4 \pm 0.2$	$1.5 \pm 0.2$
	Mean soil concentration (herding area) – grand mean	$0.44 \pm 0.02$	$0.44 \pm 0.02$	$0.44 \pm 0.02$
ERICA estimates for reindeer	Area-weighted mean (home range)	$0.69 \pm 0.04$	$0.68 \pm 0.04$	$0.68 \pm 0.04$
	Area-weighted mean (core area)	$0.76 \pm 0.04$	$0.79 \pm 0.04$	$0.83 \pm 0.04$
	Mean soil concentration (herding area) – grand mean	$0.38 \pm 0.02$	$0.38 \pm 0.02$	$0.38 \pm 0.02$
ERICA estimates for ERICA’s large mammal (deer)	Area-weighted mean (home range)	$0.60 \pm 0.03$	$0.59 \pm 0.03$	$0.59 \pm 0.03$
	Area-weighted mean (core area)	$0.66 \pm 0.04$	$0.69 \pm 0.04$	$0.72 \pm 0.04$
	Mean soil concentration (herding area) – grand mean	$0.38 \pm 0.02$	$0.38 \pm 0.02$	$0.38 \pm 0.02$

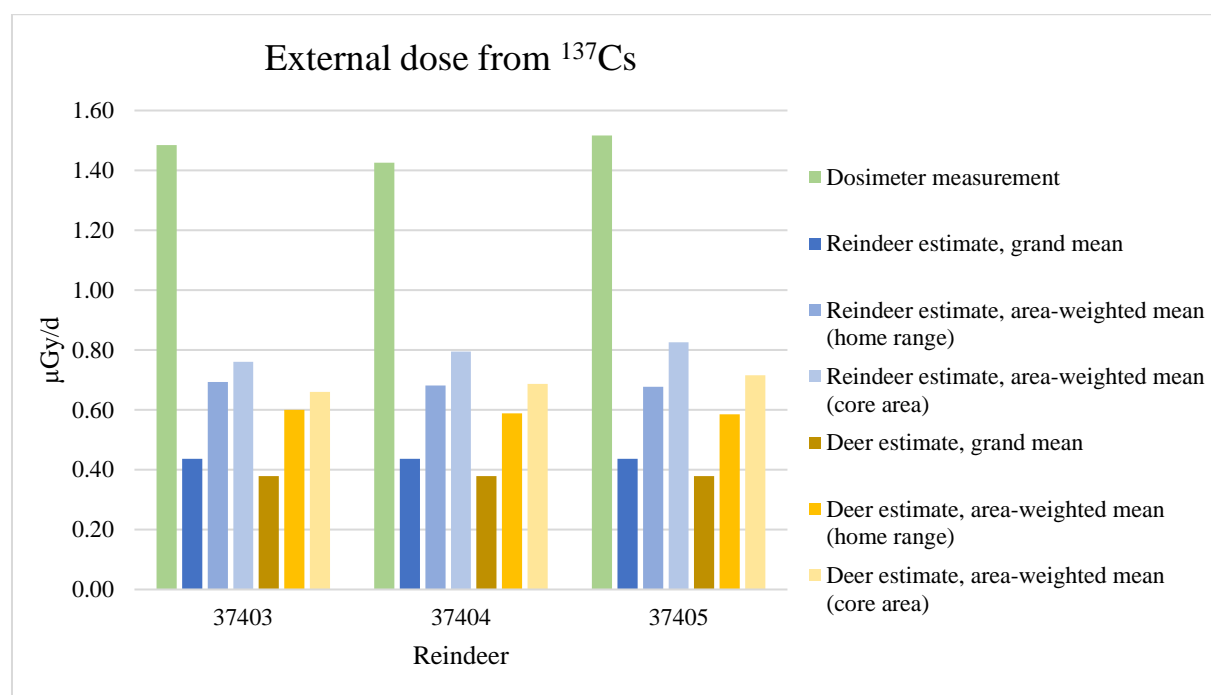


**Figure 11:** Dosimeter measurements and ERICA estimates of external  $^{137}\text{Cs}$  dose rate ( $\mu\text{Gy/d}$ ). Green bars are external  $^{137}\text{Cs}$  dose registered by dosimeters (dosimeter measurements corrected for contribution from  $^{40}\text{K}$ , cosmic radiation, and internal  $^{137}\text{Cs}$ ). The three blue bars are estimates from ERICA, using reindeer as the reference organism. The three yellow bars are estimates from ERICA, using ERICA’s large generic mammal (deer) as the reference organism. For the reindeer estimates, bars are referred to as dark blue, blue, and light blue, going from left to right in the graph. For the deer estimates, bars are referred to as dark yellow, yellow, and light yellow, going from left to right in the graph.

The daily external  $^{137}\text{Cs}$  dose rates for reindeer registered by GPS-dosimeters (green bars in Figure 11) were consistently greater than external dose estimates based on ERICA Tool and the grand mean  $^{137}\text{Cs}$  contamination levels (dark blue bars in Figure 11), with a difference of 1.0  $\mu\text{Gy/d}$ , i.e. an underestimation of 70%?. An estimate of external dose using average soil contamination level is considered conservative and should result in a dose higher than the actual dose received by the animals. One of our hypotheses was to see if this assumption is true for Norwegian reindeer, saying that “mean soil contaminant concentrations conservatively estimate individual external dose”. Our estimate from the ERICA model using grand mean is far from doses registered by GPS-dosimeters (Table 6). Consequently, it cannot be confirmed that external dose estimates based on mean soil contaminant levels is a conservative method for estimating radiation dose for these reindeer, and the hypothesis can be rejected. The same was found by Hinton et al. (2019), for wolves living in the exclusion zone around Chernobyl.

The reason for the low dose rate estimated using grand mean is that the overall herding area consists of large areas with low activity concentrations. As earlier stated, only a very small percentage of the herding area has  $^{137}\text{Cs}$  contamination levels  $>40 \text{ kBq/m}^2$  (Table 2). Therefore, the average dose rate for the area will be relatively low. However, almost all of the higher contaminated areas ( $>40 \text{ kBq/m}^2$ ) in the herding area were included in the reindeer’s home ranges (Figure 6) and made up on average 24% of the ranges (Table 2). This is the reason why estimates using grand mean represents the actual dose rate poorly.

Aramrun et al. (2019) used ERICA Tool to obtain some of the same estimates as in this study. However, Aramrun et al. (2019) used data on contaminant concentration in soil from an earlier NGU report, where  $^{137}\text{Cs}$   $\text{kBq/m}^2$  were underestimated by a factor of  $\sim 2$  compared to the updated data used here (Baranwal et al., 2020). Therefore, we have multiplied numbers from Aramrun et al. by two, to enable comparison of our data with theirs. Their estimated external  $^{137}\text{Cs}$  dose rate ( $\pm\text{SD}$ ) based on mean  $^{137}\text{Cs}$  concentration in soil for the whole herding area (grand mean) was  $0.62\pm 0.56 \mu\text{Gy/d}$ , using ERICA’s generic large mammal (deer). Our estimate using grand mean  $^{137}\text{Cs}$  concentration in soil for deer gave dose rate of  $0.38 \mu\text{Gy/d}$  (Table 6). Our dose rate was somewhat lower than Aramrun et al.’s, although their SD was rather high and included our value of 0.38. The difference is presumably caused by differences in grand mean because of variation in defined herding areas. Herding areas in the two studies overlap, but defined herding area in this thesis was bigger than in Aramrun et al. (2019). The “additional” areas in our herding area generally had low concentrations of  $^{137}\text{Cs}$ , thus lowering the grand mean and consequently also the estimate based on the grand mean.

Using area-weighted means for home ranges (blue bars in Figure 11) instead of mean soil concentration for the whole herding area gave estimates somewhat closer to real-life measurements from GPS-dosimeters (Table 6). Here, the spatial heterogeneity of  $^{137}\text{Cs}$  was accounted for by using area-weighted means for home ranges, which is a mean activity concentration value much more representable for each animal than the grand mean. However, as can be seen in Table 6 and Figure 11, estimates based on area-weighted means for home ranges were still only about half the dose measured by GPS-dosimeters, i.e. an underestimation of 53%. This could be explained by the temporal use of habitats by the reindeer. The area-weighted means do not consider exactly where in the home ranges the animals have been. Even though exact locations of the reindeer were used for the calculations of home ranges, the ranges probably include areas where the reindeer have never been. As a result, the temporal, and also spatial-temporal heterogeneity is only to some extent accounted for. But still, it represents a more realistic depiction of reindeer occurrence within the overall grazing area and better than estimates using grand mean.

Using area-weighted mean for core area in ERICA Tool gave the best estimates of external  $^{137}\text{Cs}$  dose to the reindeer, being closest to the dose rates measured by GPS-dosimeters (Table 6, Figure 11), with an underestimation of 46%. Thus, even though core areas made up only a small part of the reindeer's home ranges, their contribution to external exposure is considerable.

The fact that area-weighted mean for both home ranges and core areas resulted in estimates closer to the GPS-dosimeter measurements than the grand mean did support our second hypothesis, saying that accounting for the spatial-temporal variation of exposure, using area-weighted mean soil contamination levels within each animal's home range, gives a more realistic radiation dose estimate. These results demonstrate the importance of accounting for spatial and temporal variability of contaminant levels and animal habitat preferences when simulating exposure to biota.

Dose estimations performed with ERICA's generic large mammal (deer) were generally lower than for the "new" reindeer organism we specifically derived based on organism size (Table 6). ERICA's generic large mammal is a woodland deer with a mass of 245 kg, measuring 130 cm in length, 60 cm in width, and 60 cm in height (ICRP, 2008). Note that the height of 60 cm is height of the body itself, not the height from the ground up to the shoulders (as the height given for our reindeer reference organism is). A red deer, one of the larger deer species, with a weight of 245 kg typically has a height of 120-135 cm (Langvatn, 2021). Red deer are considerably larger than our reindeer, which has a mass of only 100 kg and height of 90 cm. External DCCs

increase as an organism's size/mass decreases (Aramrun et al., 2019; Saito et al., 2012; Ulanovsky, 2014), consequently leading to increased dose rate as size decreases (based on the same activity concentration). This explains why estimates of external dose rate to reindeer were higher than external dose rates to deer.

In addition to mass, the height of the organism will affect received external radiation dose (Ulanovsky, 2014). Compared to our reindeer (90 cm), the deer (120-135 cm) stands taller, so its body is situated further away from the ground. Meaning, the deer is further away from the  $^{137}\text{Cs}$  source (soil). On its way from soil to an animal, gamma radiation can scatter or be adsorbed, by for example vegetation. The further away from the soil an organism is, the greater are chances for radiation to be scattered or adsorbed before reaching its body. Consequently, a deer will receive a slightly lower radiation dose from radionuclides in soil than reindeer.

### *Snow Cover*

Snow and ice cover can affect radiation dose received by organisms. It can function as a shield, attenuating radiation coming from radionuclides in soil (Ishizaki et al., 2016; Offenbacher & Colbeck, 1991). For reindeer living in Norwegian mountain areas, snow cover can be quite deep during winter. Also, winter can be long, with snow/ice on the ground for major parts of the year. This factor can reduce the radiation dose received by reindeer, compared to if there were no snow.

It is hard to say if this shielding effect of snow/ice can be seen in our dosimeter data. Looking at Figure 13 (integrated dose rates for 5 days) we see that dose rates increase somewhat towards the end of the measuring period. Snow cover in spring and early summer could have led to attenuation of radiation from  $^{137}\text{Cs}$ , reducing dose rates in this period. However, we do not have information about snow conditions in the area from spring/summer of 2019. But, 2019 was a year with high temperatures and an unusually early snow melting (Johansen et al., 2019; NVE, 2020). Thus, reduction of snow cover is most likely not the reason for the dose rate increase for the reindeer in late summer.

The attenuating effect of snow and ice cover is not considered in ERICA Tool (Aramrun et al., 2019). It follows that the model might overestimate dose for organisms experiencing snow cover during a year. However, our model estimates were all lower than GPS-dosimeter measurements.

## 4.4 Information Obtained When Using Active Dosimeters

The use of active dosimeters gave us real-time dose rate data that are hard to obtain in any other way. An active dosimeter registers dose at set intervals, in this case every hour, as opposed to a passive dosimeter, which Aramrun et al. (2019) used in their study, where dose was integrated for the whole period the dosimeter was attached to the animal (11 months). Active dosimeters can thus give information about the variation in dose received by animals over time, whereas such fine scale data are not possible with passive dosimeters. Although not examined in this work, active dosimeters can also be used to more precisely link radiation dose to potential effects and obtain better dose rate-response relationships. This would not be as feasible using passive dosimeters.

### 4.4.1 Variation in Dose Rate

Hourly doses from dosimeters were integrated into daily doses. Daily doses ranged from 1-5  $\mu\text{Gy}/\text{d}$  for #37403 (Figure 12 (a)), and 2-5  $\mu\text{Gy}/\text{d}$  for #37404 and #37405 (Figure 12 (b, c)). These dose rates were not corrected for cosmic radiation, internal  $^{137}\text{Cs}$  and  $^{40}\text{K}$ , but do still show the variation in daily dose received by the reindeer. In the wolf-study by Hinton et al. (2019), variations in external  $^{137}\text{Cs}$  dose rates were considerably greater than in our study, being at most a  $\sim 30$  fold range over a 12-day period for one of the wolves. While for the reindeer, maximum range in variation were fivefold. This implies that the wolves might had a higher variation in activity concentrations and/or more extreme  $^{137}\text{Cs}$  concentrations within the landscape of their home range than the reindeer. The more extreme  $^{137}\text{Cs}$  concentrations in Chernobyl are clearly illustrated when comparing the wolves' external (GPS-dosimeter measurements only corrected for contribution from internal exposure) dose rate ( $\sim 50 \pm 36 \mu\text{Gy}/\text{d}$  on average) to the reindeers ( $\sim 2.5 \mu\text{Gy}/\text{d}$  n average) (Hinton et al., 2019).

The range in dose rates shows how the spatial-temporal heterogeneity of contaminant-animal interactions affect the dose received. With an even distribution of radionuclides there would not have been such big differences in dose between days. The only variance would then come from cosmic radiation, dependent on altitude on the location of the animal (which we found to be about  $0.4 \mu\text{Gy}/\text{d}$  for the reindeer), and internal contribution, depending on what the animal has eaten. But with an uneven distribution of radionuclides across the landscape and different amounts of time spent in different areas, there will obviously be variation in dose rates over short time intervals. Variation in dose rates over time cannot be obtained from passive dosimeters.

When evaluating risk related to radioactive radiation it is useful to know the variation in dose over time. Damage increases with increasing dose rate (Choppin et al., 2013), thus it is important to know maximum doses and for how long an organism has been exposed to that dose. An average dose rate obtained from passive dosimeters will not give any information about this. Concerning our reindeer, their maximum dose rate was 5  $\mu\text{Gy/d}$  for 3, 6, and 4 days for #37403, #37404, and #37405, respectively (Figure 12). So, they did not experience very high dose rates, and not for long periods. Not looking at the variation, but only average values of dose rate might lead to the wrong decisions being made, for example when there is a need for actions on the occasion of accidental discharge of radioactive materials.

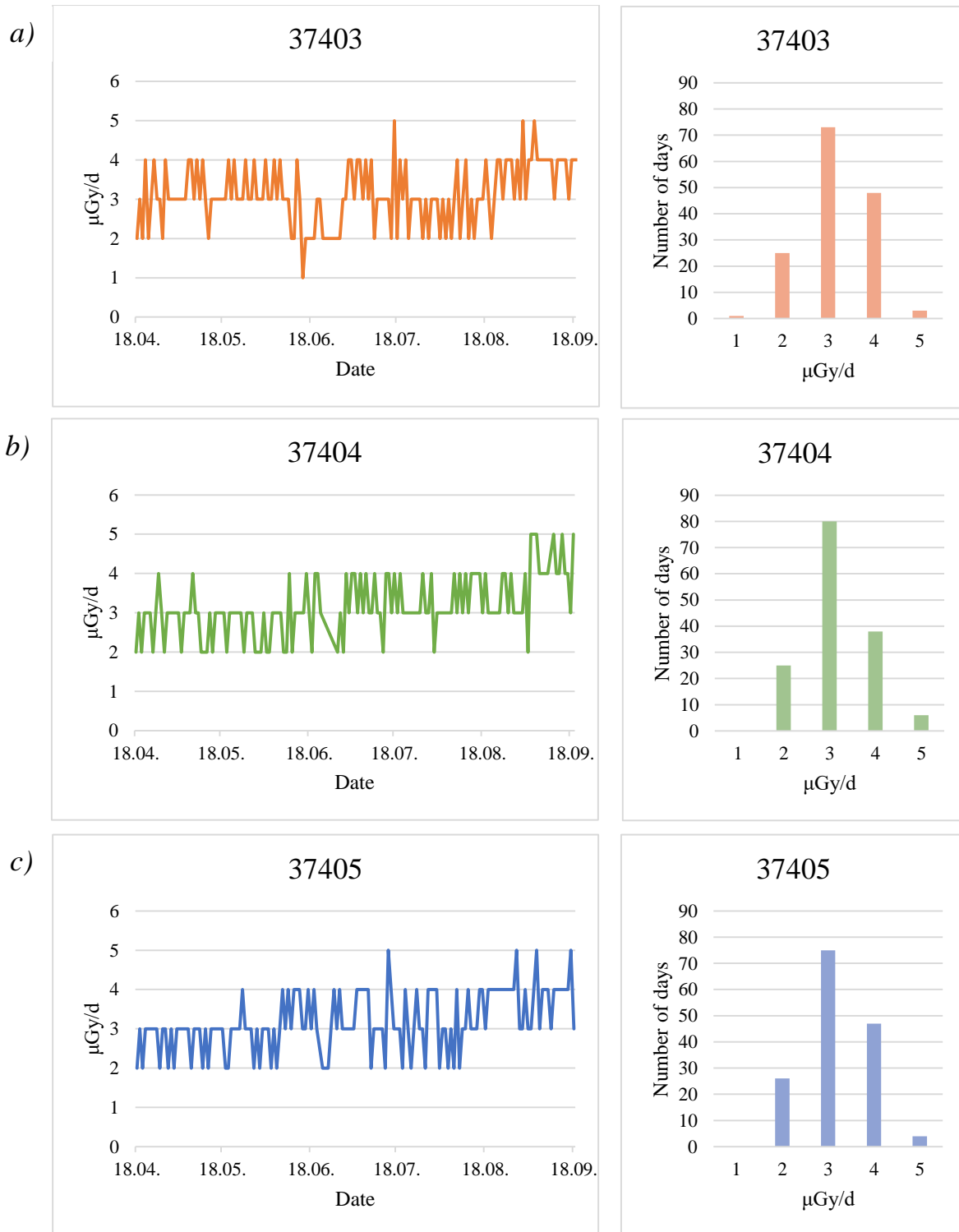


**Figure 12:** Variation (to the left) and distribution (to the right) of dose rate ( $\mu\text{Gy/d}$ ) throughout the study period for reindeer 37403 (a), 37404 (b), and 37405 (c).



In Figure 13 daily doses were integrated into 5-day doses, to make it easier to identify any potential trends and periodical changes in the reindeer's received dose. Trend lines from the time series regression analysis demonstrate an increase in dose rate towards the end of the study period. Trend lines had MSE of 2.9, 1.1, and 3.0 for #37403, #37404, and #37405, respectively.

Looking at GPS locations for mid to late August and early to mid-September many of them occur in the highly contaminated parts of the reindeer's home ranges. Consequently, we observe an increase in daily dose towards the end of the study period, which was most apparent for #37404 and #37405. Following the concentrated activity, parts of core areas for #37404 and #37405 are situated in these highly contaminated areas (Figure 17 and Figure 18, Appendix B), thus the reindeer were occupying areas with relatively high  $^{137}\text{Cs}$  contamination in their core area. Area-weighted  $^{137}\text{Cs}$  activity concentration means for core areas were higher than for home ranges (Table 3) for all three reindeer, but the difference was most apparent for #37404 and #37405.

Core areas also had a slightly higher average altitude than home ranges for all three reindeer (Table 8, Appendix B), which can be one of the reasons why the animals seek these areas in late summer. Food availability and quality changes with altitude and seasons. At higher altitude plants are at an earlier grow stage compared to lower altitudes because spring starts later at elevated altitudes. Since shoots and younger plant parts, typically available early in the growing season, are preferred over older, more mature ones by most herbivores, including mammalian herbivores (e.g. Coley, 1980; Gong et al., 2020; Lowman, 1992), it follows that the reindeer might seek higher elevations towards the end of summer and the autumn (July-August-September). A tendency for reindeer and other cervids to follow the emergence of fresh plant shoots has been observed also in earlier studies (e.g. Marchinton & Hirth, 1984; Oosenbrug & Theberge 1980; Skogland, 1984).

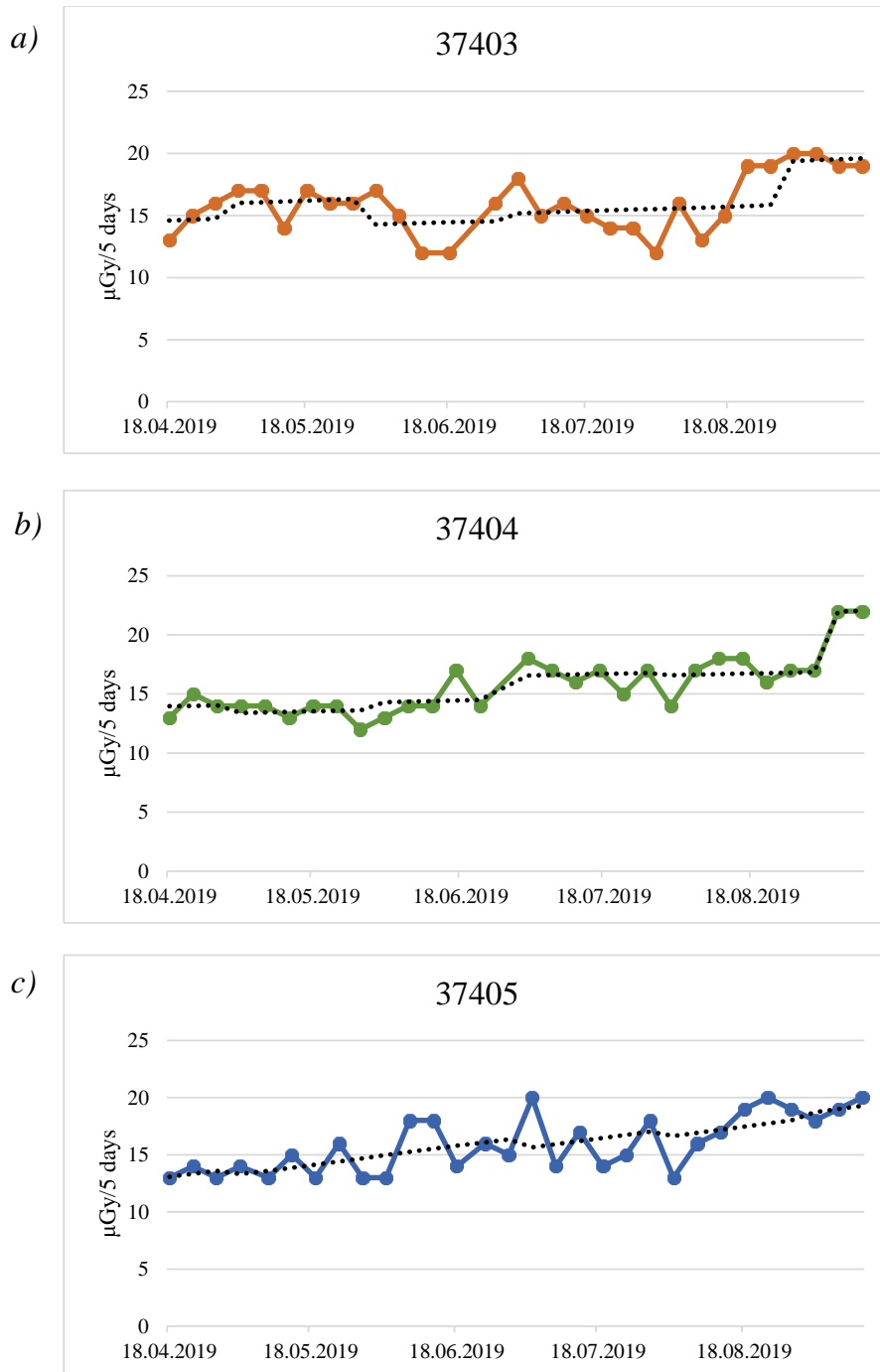


**Figure 13:** Variation in dose rate, integrated into 5-day intervals, over time for reindeer 37403 (a), 37404 (b), and 37405 (c). Daily doses are summed up for five days and presented as  $\mu\text{Gy}/5 \text{ days}$ , shown here by coloured (unbroken) lines. The black, dotted lines are obtained by time series regression analysis and present the trend in dose rate with time. Mean squared error was 2.9, 1.1, and 3.0 for #37403, #37404, and #37405, respectively.

#### 4.4.2 Using Reindeer as a “Biotic Contaminant Mapper”

We briefly looked at the potential of using reindeer as a “biotic contaminant mapper”, providing data on radionuclide concentrations in soil within area not mapped using fly-over data from aircraft. By comparing measured external  $^{137}\text{Cs}$  dose from GPS-dosimeters with  $^{137}\text{Cs}$  concentration levels ( $\text{kBq}/\text{m}^2$ ) from the aerial survey we can look for correlations between the two variables. This was done for the whole study period for all three reindeer. Some of the hourly GPS locations were removed from the dataset, as mentioned earlier, because they were located outside of the area mapped for radionuclides. Therefore, when only daily dose measurements with corresponding 24 hours are used for these calculations and plots, some dates are missing. However, there were still more than 130 dates having a daily dose with corresponding 24 hours, so data were still representable for what we want to investigate.

Correlation between external  $^{137}\text{Cs}$  dose rates and levels of  $^{137}\text{Cs}$  in soil and associated  $r_s$  values are shown in Figure 14, Figure 15, and Figure 16 for reindeer 37403, 37404, and 37405, respectively. The graphs are quite similar, showing little variation between animals. Little variation is also shown in several of the results presented earlier. One of the major reasons for this is that reindeer are gregarious animals, clearly illustrated by their almost completely overlapping home ranges (Figure 6). As can be seen in the plots (Figure 14, Figure 15, and Figure 16), points are distributed in “layers”. This is because daily doses registered by GPS-dosimeters are given as whole numbers and the corrections (cosmic radiation, internal  $^{137}\text{Cs}$ , and  $^{40}\text{K}$  in soil) are relatively similar for most of the points.

We expect dose rate to increase with the concentration of  $^{137}\text{Cs}$  in soil, and thus the correlation between the two to be strong. For all three reindeer, doses  $>2.5 \mu\text{Gy}/\text{d}$  only occur in areas with  $^{137}\text{Cs}$  levels  $>30 \text{kBq}/\text{m}^2$ . Doses  $<1 \mu\text{Gy}/\text{d}$  only occur in areas with  $^{137}\text{Cs}$  levels  $<40 \text{kBq}/\text{m}^2$  for #37403 and #37405. The same is almost also true for #37404, with only a few doses  $<1 \mu\text{Gy}/\text{d}$  above  $40 \text{kBq}/\text{m}^2$ . These observations corroborate the trend of increasing dose rate with increasing  $^{137}\text{Cs}$  levels in soil. The  $r_s$  values (Spearman correlation coefficients) are measures of the strength of correlation between registered external  $^{137}\text{Cs}$  dose rate and  $^{137}\text{Cs}$  concentration in soil, ranging from -1 to 1, with  $r_s=1$  being a complete correlation. Here,  $r_s$  values of 0.51, 0.44, and 0.57 for #37403, #37404, and #37405, respectively, indicate moderate correlation between the two variables. Large variations in dose rates for given contaminant levels ( $\text{kBq}/\text{m}^2$ ) and vice versa (Figure 14, Figure 15, and Figure 16) are the reason the correlations were not stronger.

The idea of mapping  $^{137}\text{Cs}$  in soil using GPS-dosimeters and reindeer did not work well in our case. One reason for this could be that dose rates and  $^{137}\text{Cs}$  levels in soil were too low and had too little variation. With a broader range of dose rates and  $^{137}\text{Cs}$  concentrations in soil it is plausible the increasing trend would have been clearer. Also, because of the relatively low  $^{137}\text{Cs}$  activity concentrations in soil, doses registered by GPS-dosimeters were close to the detection limit of the dosimeter, contributing to greater uncertainty. In the Chernobyl wolf study, Hinton et al. (2019) reported a clear correlation ( $r^2=0.89$ ) between area-weighted contamination densities in the wolves' home ranges and the external exposures measured with GPS-dosimeters. The correlation was even better for area-weighted contamination densities in the wolves' core area ( $r^2=0.99$ ), which agrees with our findings of the importance of accounting for the temporal use of habitat by animals. The strong correlations shown in (Hinton et al., 2019) illustrate that higher contamination concentrations and broader ranges of dose rates can give a much clearer correlation.

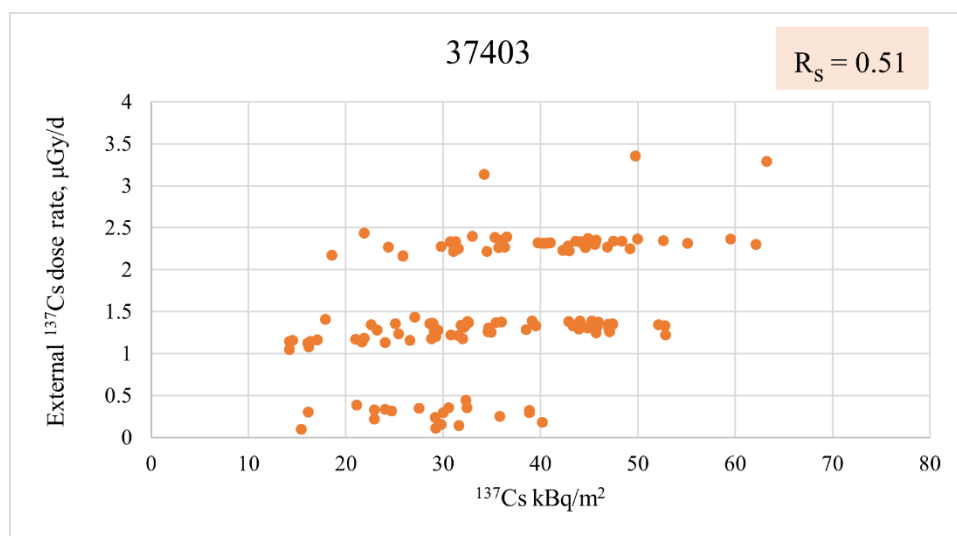


**Figure 14:** Plot of external  $^{137}\text{Cs}$  dose rates ( $n=132$ ) registered by GPS-dosimeters and levels of  $^{137}\text{Cs}$  in soil from airborne radiometric survey for reindeer 37403. The Spearman correlation coefficient,  $r_s$ , is obtained from a Spearman correlation test.  $R_s = 0.51$  indicate a moderate correlation.

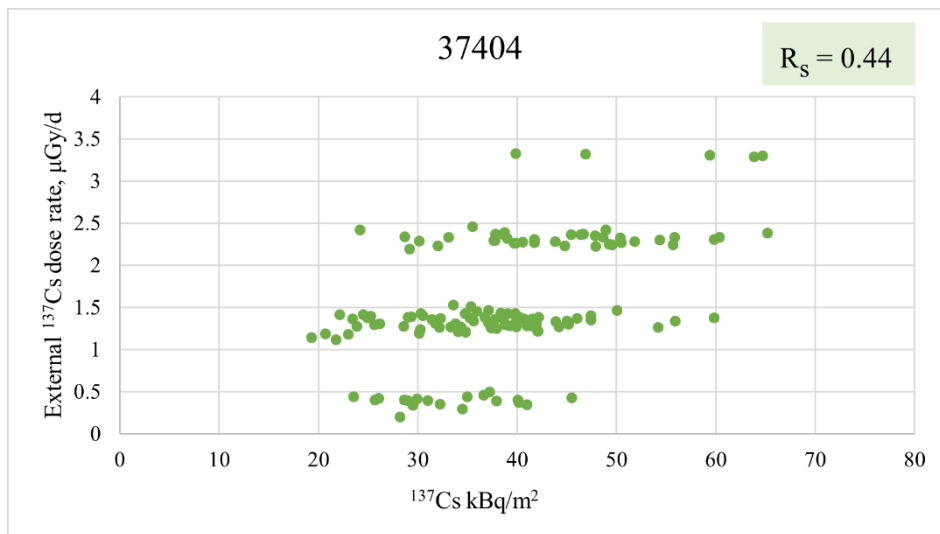


**Figure 15:** Plot of external  $^{137}\text{Cs}$  dose rates ( $n=132$ ) registered by GPS-dosimeters and levels of  $^{137}\text{Cs}$  in soil from airborne radiometric survey for reindeer 37404. The Spearman correlation coefficient,  $r_s$ , is obtained from a Spearman correlation test.  $R_s = 0.44$  indicate a moderate correlation.

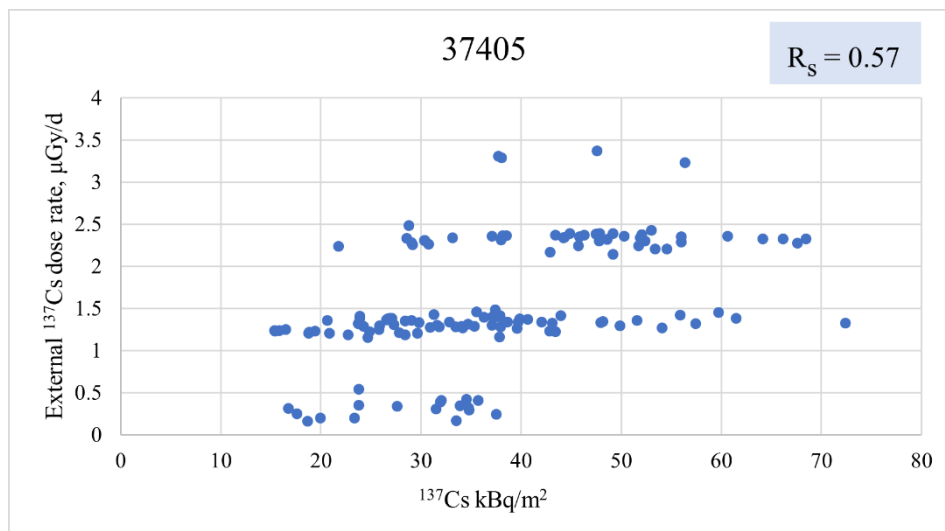


**Figure 16:** Plot of external  $^{137}\text{Cs}$  dose rates ( $n=132$ ) registered by GPS-dosimeters and levels of  $^{137}\text{Cs}$  in soil from airborne radiometric survey for reindeer 37405. The Spearman correlation coefficient,  $r_s$ , is obtained from a Spearman correlation test.  $R_s = 0.57$  indicate a moderate correlation.

## 4.5 Uncertainties

Several factors contribute to the uncertainty associated with radiation dose measurements and estimates in this thesis. An overview of relative standard deviations (RSD) is presented in Table 7. Uncertainties are always important to consider and include in calculations and results, as they give an indication on the accuracy of measurements and estimates. Only the RSDs in Table 7 are included and presented in the results of this thesis. Other uncertainty factors can also be relevant but are not considered here, such as uncertainties connected to soil water content, dimensions of the reference organisms, snow-/ice cover, and cosmic radiation.

For ERICA estimates the only RSD of concern included was from the mapping of  $^{137}\text{Cs}$ . For the corrected GPS-dosimeter measurements, RSD for both dosimeters measurements, internal  $^{137}\text{Cs}$  activity concentration, and mapping of K were included in a combined uncertainty, because all the individual uncertainties did contribute to the uncertainty of the corrected measurements. GPS location errors will be an uncertainty factor affecting size and location of home ranges and core areas. The accuracy of locations registered by GPSs depends among other things on satellite coverage and vegetation (Grinderud et al., 2016). GPS location errors of  $4.2 \pm 8.0$  m in open field,  $8.7 \pm 9.0$  m in birch forest, and  $8.9 \pm 11.4$  m in pine forest were reported by Hinton et al. (2019), using similar GPS-dosimeters as in the current work. These errors are expected to be in the range of what Hinton et al. reported, but were not quantified and included in calculations in our study. Overall, our uncertainties are relatively low. However, as previously mentioned, there are also other uncertainty factors than the ones discussed here that are current.

**Table 7:** Relative standard deviations (RSD) for the quantified uncertainties contributing to the overall uncertainty of our results. For mapping of K and  $^{137}\text{Cs}$  5% (maximum value) was used as RSD for calculations of uncertainties. In addition to the quantified uncertainties there are other uncertainties contributing to the overall uncertainty of both GPS-dosimeter measurements and ERICA estimates.

	GPS-dosimeter measurements (RSD %)	ERICA estimates (RSD %)
<b>Dosimeter</b>	5%	-
<b>Internal <math>^{137}\text{Cs}</math> activity concentration</b>	3%	-
<b>Mapping of K</b>	$\leq 5\%$	-
<b>Mapping of <math>^{137}\text{Cs}</math></b>	-	$\leq 5\%$
<b>Unknown uncertainties</b>	x	x

## 4.6 Future Research

More research is needed on this subject, to further test hypotheses of interest. Our sample size was very small, only looking at data from three individuals. Future research should include larger sample sizes and other wild species and areas with different contaminant concentrations. More empirical data on dose rates will be of great value and are needed for validation of ERICA Tool and other simulation models, to obtain knowledge about accuracy and utility of the models. Information about what is needed to improve dose estimates and how to include it in models is desirable, so that we can use them for management and ecological risk assessments with confidence.

The idea of using reindeer or other animals for contaminant mapping might have potential and should therefore be further researched. In the present work, levels of  $^{137}\text{Cs}$  in soil and dose rates were rather low. Areas with higher maximum contaminant concentration should be used in future studies, to obtain a wider spectrum of dose rates and contaminant levels when this can make possible correlations clearer.

By replacing dosimeters with gamma spectrometers one could obtain information not only on the total dose of gamma radiation, but also on which radionuclides the radiation comes from. A gamma spectrum enables distinction of different gamma sources, and thus identification of radionuclides present. Coupled to a GPS, the gamma spectrometer could potentially be used to identify and map gamma emitting materials, from both natural and anthropogenic origin, and further study received gamma radiation dose in free-ranging wildlife.

## 5 Conclusions

Radioactive fallout from the Chernobyl accident in 1986 still affects animal husbandry in some areas of Norway, among others Jotunheimen. External  $^{137}\text{Cs}$  radiation dose in semi-domesticated reindeer in the Jotunheimen area was measured by GPS-dosimeters and compared to estimated external  $^{137}\text{Cs}$  radiation dose based on soil contamination using model simulations within the ERICA Tool. The heterogeneous distribution of  $^{137}\text{Cs}$  and the temporal use of habitats make it challenging to simulate external  $^{137}\text{Cs}$  radiation dose in free-ranging animals, like reindeer. Herein we have tested the hypothesis that using mean soil contaminant concentrations (grand mean) give conservative estimates of individual external dose, using ERICA Tool. Estimates from ERICA Tool using mean soil contamination concentration (grand mean for herding area) underestimated by 70% the external dose measured with GPS-dosimeters worn on animals, and the hypothesis was therefore rejected. Accounting for the spatiotemporal heterogeneity by using area-weighted means for home range and core area improved the estimates somewhat, with underestimations of 53% and 46%, respectively, when compared to GPS-dosimeter measurements. Therefore, our second hypothesis, stating that accounting for spatio-temporal variation of exposure gives a more realistic radiation dose estimate, can to some extent be confirmed. This emphasises the importance of testing estimation models against empirical field measurements. Models, like ERICA Tool, are widely used in ecological risk assessments and is a useful tool in the case of accidents or other emergencies where radionuclides are emitted. Hence, validation of such models is of great value and importance.

We also looked briefly into the additional information obtained when using active dosimeters instead of passive dosimeters. Using reindeer wearing GPS-dosimeters to map  $^{137}\text{Cs}$  in soil did not work well in our study, only moderate correlations were identified. This should be investigated in areas with higher contamination concentrations and broader range of received radiation doses, to maybe obtain clearer results.



## References

- Anderson, D., Kaneko, S., Harshman, A., Okuda, K., Toshito, T., Chinn, S., Beasley, J. C., Nanba, K., Ishiniwa, H. & Hinton, T. G. (2022). Radiocesium accumulation and germline mutations in chronically exposed wild boar from Fukushima, with radiation doses to human consumers of contaminated meat. *Environ Pollut*: 119359-119359. doi: 10.1016/j.envpol.2022.119359.
- Aramrun, K., Beresford, N. A., Skuterud, L., Hevrøy, T. H., Drefvelin, J., Bennett, K., Yurosko, C., Phruksarojanakun, P., Esoa, J., Yongprawat, M., et al. (2019). Measuring the radiation exposure of Norwegian reindeer under field conditions. *Sci Total Environ*, 687: 1337-1343. doi: 10.1016/j.scitotenv.2019.06.177.
- Baranwal, V. C., Ofstad, F., Rønning, J. S. & Watson, R. J. (2011). *Mapping of caesium fallout from the Chernobyl accident in the Jotunheimen area*, 2011.062: Geological Survey of Norway (NGU).
- Baranwal, V. C., Stampolidis, A., Koziel, J., Watson, R. J. & Rønning, J. S. (2020). *Reprocessing of airborne gamma-ray spectrometry data in Norway for mapping of Cs-137 deposition from the Chernobyl accident*, 2019.039: Geological Survey of Norway (NGU).
- Beresford, N. A., Wright, S. M., Barnett, C. L., Wood, M. D., Gaschak, S., Arkhipov, A., Sazykina, T. G. & Howard, B. J. (2005). Predicting radionuclide transfer to wild animals: an application of a proposed environmental impact assessment framework to the Chernobyl exclusion zone. *Radiation and environmental biophysics*, 44: 161-168. doi: 10.1007/s00411-005-0018-z.
- Beresford, N. A., Gaschak, S., Barnett, C. L., Howard, B. J., Chizhevsky, I., Strømman, G., Oughton, D. H., Wright, S. M., Maksimenko, A. & Copplestone, D. (2008). Estimating the exposure of small mammals at three sites within the Chernobyl exclusion zone – a test application of the ERICA Tool. *J Environ Radioact*, 99 (9): 1496-1502. doi: 10.1016/j.jenvrad.2008.03.002.
- Biørnstad, L. (2014). Atombombe-restene i Norge. Available at: <https://forskning.no/atombombe-fysikk/atombombe-restene-i-norge/525322>.
- Brown, J. E., Alfonso, B., Avila, R., Beresford, N. A., Copplestone, D., Pröhl, G. & Ulanovsky, A. (2008). The ERICA Tool. *Journal of Environmental Radioactivity*, 99: 1371-1383. doi: 10.1016/j.jenvrad.2008.01.008.
- Choppin, G., Liljenzin, J.-O., Rydberg, J. & Ekberg, C. (2013). *Radiochemistry and Nuclear Chemistry*. 4th ed.: Academic Press.
- Cinelli, G., Gruber, V., De Felice, L., Bossew, P., Hernandez-Ceballos, M. A., Tollefsen, T., Mundigl, S. & De Cort, M. (2017). European annual cosmic-ray dose: estimation of population exposure. *Journal of maps*, 13 (2): 812-821. doi: 10.1080/17445647.2017.1384934.
- Coggle, J. E., Lambert, B. E. & Moores, S. R. (1986). Radiation effects in the lung. *Environmental health perspectives*, 70: 261-291. doi: 10.2307/3430363.
- Coley, P. D. (1980). Effects of leaf age and plant life history patterns on herbivory. *Nature*, 284: 545-546. doi: 10.1038/284545a0.
- Cui, L., Orita, M., Taira, Y. & Takamura, N. (2020). Radiocesium concentrations in wild boars captured within 20 km of the Fukushima Daiichi Nuclear Power Plant. *Sci Rep*, 10 (1): 9272. doi: 10.1038/s41598-020-66362-6.
- DOE (U.S. Department of Energy). (2019). *DOE Standard: A graded approach for evaluating radiation doses to aquatic and terrestrial biota*, DOE-STD-1153-2019. Washington: U.S. Department of Energy.
- Eckl, P., Hofmann, W. & Türk, R. (1986). Uptake of natural and man-made radionuclides by lichens and mushrooms. *Radiat Environ Biophys*, 25 (1): 43-54. doi: 10.1007/BF01209684.
- Eikermann, I., Bye, K. & Sletten, H. (1990). Seasonal variation of cesium 134 and cesium 137 in semidomestic reindeer in Norway after the Chernobyl accident. *Rangifer* (Special Issue No. 3): 35-38. doi: 0.7557/2.10.3.818.
- EPA (U.S. Environmental Protection Agency). *Ecological risk assessment*: United States Environmental Protection Agency. Available at: <https://www.epa.gov/risk/ecological-risk-assessment> (accessed: 27.04.22).

- EPA (U.S. Environmental Protection Agency). (1996a). *Soil Screening Guidance: User's Guide*, EPA/540/R-96/018. Washington DC (U.S.): U.S. Environmental Protection Agency, Office of Emergency and Remedial Response.
- EPA (U.S. Environmental Protection Agency). (1996b). *Soil Screening Guidance: Technical Background Document*, EPA/540/R95/128. Washington DC (U.S.): U.S. Environmental Protection Agency, Office of Solid Waste and Emergency Response.
- EPA (U.S. Environmental Protection Agency). (2008). *Technologically enhanced naturally occurring radioactive materials from uranium mining. Volum 1: Mining and reclamation background. Volum 2: Investigation of potential health, geographic, and environmental issues of abandoned uranium mines.*, EPA 402-R-08-005: U.S. Environmental Protection Agency, Office of Radiation and Indoor Air.
- EPA (U.S. Environmental Protection Agency). (2021). *Radionuclide Basics: Cesium-137*: U.S. Environmental Protection Agency. Available at: <https://www.epa.gov/radiation/radionuclide-basics-cesium-137#cesiumhealth> (accessed: 01.02.22).
- Fleming, C. H. & Calabrese, J. M. (2017). A new kernel density estimator for accurate home-range and species-range area estimation. *Methods in Ecology and Evolution*, 8: 571-579. doi: 10.1111/2041-210X.12673.
- Fremstad, J. J. (2019). *Godt soppår ga mer radioaktivitet i villrein*: Norsk institutt for naturforskning (NINA). Available at: <https://www.nina.no/About-NINA/News/article/godt-sopp-229-r-ga-mer-radioaktivitet-i-villrein> (accessed: 02.02.22).
- Geras'kin, S. A., Fesenko, S. V. & Alexakhin, R. M. (2008). Effects of non-human species irradiation after the Chernobyl NPP accident. *Environ Int*, 34 (6): 880-897. doi: 10.1016/j.envint.2007.12.012.
- Gjelsvik, R., Komperød, M., Brittain, J. E., Eikermann, I. M., Gaare, E., Gwynn, J., Holmstrøm, F., Jensen, L. K., Kållås, J. A., Møller, B., et al. (2014). *Radioaktivt cesium i norske landområder og ferskvannssystemer. Resultater fra overvåkning i perioden 1986-2013*, 2014:9: Statens strålevern (Norwegian Radiation Protection Authority).
- Gong, W.-C., Liu, Y.-H., Wang, C.-M., Chen, Y.-Q., Martin, K. & Meng, L.-Z. (2020). Why Are There so Many Plant Species That Transiently Flush Young Leaves Red in the Tropics? *Frontiers in Plant Science*, 11. doi: 10.3389/fpls.2020.00083.
- Grinderud, K., Haavik-Nilsen, A. C., Bjerke, H., Sanderud, Ø., Ulveseth, P. G., Mauseth, Ø., Nilsen, S., Fjetland, M., Steffensen, A. & Richardsen, I. (2016). *GIS : geografiens språk i vår tidsalder*. 2. utg. ed. Geografiens språk i vår tidsalder. Bergen: Fagbokforl.
- Gäfvvert, T., Boson, J., Karhunen, T., Jónsson, G., Juul Krogh, S., Drefvelin, J., Hetland, P. O., Skuterud, L., Reppenhausen Grim, P., Smolander, P., et al. (2016). *Nordic in Situ Gamma Intercomparison. Final Report from NKS-B NISI Project (Contract: AFT/B(16)2), NKS-377*. Roskilde, Denmark: NKS (Nordic Nuclear Safety Research) Secretariat.
- Harmelin-Vivien, M., Bodiguel, X., Charmasson, S., Loizeau, V., Mellon-Duval, C., Tronczynski, J. & Cossa, D. (2012). Differential biomagnification of PCB, PBDE, Hg and Radiocesium in the food web of the European hake from the NW Mediterranean *Marine Pollution Bulletin*, 64 (5): 974-983. doi: 10.1016/j.marpolbul.2012.02.014.
- Heinrich, G. (1992). Uptake and transfer factors of <sup>137</sup>Cs by mushrooms. *Radiat Environ Biophys*, 31 (1): 39-49. doi: 10.1007/BF01211511.
- Hinton, T. G., Garnier-Laplace, J., Vandenhove, H., Dowlall, M., Adam-Guillermin, C., Alonzo, F., Barnett, C., Beaugelin-Seiller, K., Beresford, N. A., Bradshaw, C., et al. (2013). An invitation to contribute to a strategic research agenda in radioecology. *J Environ Radioact*, 115: 73-82. doi: 10.1016/j.jenvrad.2012.07.011.
- Hinton, T. G., Byrne, M. E., Webster, S. & Beasley, J. C. (2015). Quantifying the spatial and temporal variation in dose from external exposure to radiation: a new tool for use on free-ranging wildlife. *Journal of Environmental Radioactivity*, 145: 58-65. doi: 10.1016/j.jenvrad.2015.03.027.
- Hinton, T. G., Byrne, M. E., Webster, S. C., Love, C. N., Broggio, D., Trompier, F., Shamovich, D., Horloogin, S., Lance, S. L., Brown, J., et al. (2019). GPS-coupled contaminant monitors on free-ranging Chernobyl wolves challenge a fundamental assumption in exposure assessments. *Environment International*, 133. doi: 10.1016/j.envint.2019.105152.

- IAEA (International Atomic Energy Agency). (1992). *Effects of Ionizing Radiation on Plants and Animals at Levels Implied by Current Radiation Protection Standards*, 332. Vienna (Austria).
- IAEA (International Atomic Energy Agency). (1999). *Protection of the environment from the effects of ionizing radiation: A report for discussion*, IAEA-TECDOC-1091. Vienna, Austria: International Atomic Energy Agency.
- IAEA (International Atomic Energy Agency). (2004). *Live Chart of Nuclides*: International Atomic Energy Agency. Available at: <https://www-nds.iaea.org/relnsd/vcharthtml/VChartHTML.html> (accessed: 11.05.22).
- IAEA (International Atomic Energy Agency). (2007). *Live Chart of Nuclides*: International Atomic Energy Agency. Available at: <https://www-nds.iaea.org/relnsd/vcharthtml/VChartHTML.html> (accessed: 11.05.22).
- IAEA (International Atomic Energy Agency). (2017). *Live Chart of Nuclides*: International Atomic Energy Agency. Available at: <https://www-nds.iaea.org/relnsd/vcharthtml/VChartHTML.html> (accessed: 13.05.22).
- ICRP (International Commission on Radiological Protection). (1979). Limits for Intakes of Radionuclides by Workers. ICRP Publication 30 (Part 1). *Annals of the ICRP*, 2 (3-4).
- ICRP (International Commission on Radiological Protection). (2008). *Environmental Protection: The Concept and Use of Reference Animals and Plants*. ICRP Publication 108. Annals of the ICRP: International Commission on Radiological Protection.
- Ishizaki, A., Sanada, Y., Mori, A., Imura, M., Ishida, M. & Munakata, M. (2016). Investigation of Snow Cover Effects and Attenuation Correction of Gamma Ray in Aerial Radiation Monitoring. *Remote sensing (Basel, Switzerland)*, 8 (11): 892. doi: 10.3390/rs8110892.
- Joel, E. S., Maxwell, O., Adewoyin, O. O., Ehi-Eromosele, C. O., Embong, Z. & Oyawoye, F. (2018). Assessment of natural radioactivity in various commercial tiles used for building purposes in Nigeria. *MethodsX*, 5: 8-19. doi: 10.1016/j.mex.2017.12.002.
- Johansen, S. A., Lusæter, E. & Sandholt, R. K. (2019). *Samtlige sommerskisentre har stengt: -Snøen smelter bort*: NRK (Norsk rikskringkasting). Available at: <https://www.nrk.no/innlandet/samtlige-sommerskisentre-har-stengt-pa-grunn-av-stor-snosmelting-1.14642793> (accessed: 09.04.22).
- Kamiya, K., Ozasa, K., Akiba, S., Niwa, O., Kodama, K., Takamura, N., Zaharieva, E. K., Kimura, Y. & Wakeford, R. (2015). Long-term effects of radiation exposure on health. *The lancet*, 386 (9992): 469-478. doi: 10.1016/S0140-6736(15)61167-9.
- Ketterer, M. E., Hafer, K. M., Link, C. L., Kolwaite, D., Wilson, J. & Mietelski, J. W. (2004). Resolving global versus local/regional Pu sources in the environment using sector ICP-MS. *Journal of analytical atomic spectrometry*, 19 (2): 241-245. doi: 10.1039/b302903d.
- Kofstad, P. K. & Pedersen, B. (2021). *Cesium*: Store norske leksikon. Available at: <https://snl.no/cesium> (accessed: 31.01.22).
- Kónya, J. & Nagy, N. M. (2012). Radioactive decay. In *Nuclear and radiochemistry*, pp. 49-82: Elsevier.
- Krivolutzkii, D. & Pokarzhevskii, A. (1992). Effects of radioactive fallout on soil animal populations in the 30 km zone of the Chernobyl atomic power station. *Science of the total environment*, 112 (1): 69-77. doi: 10.1016/0048-9697(92)90239-O.
- Langvatn, R. (2021). *Hjort*: Store norske leksikon. Available at: <https://snl.no/hjort> (accessed: 20.04.22).
- Langvatn, R. (2022). *Rein*: Store norske leksikon. Available at: <https://snl.no/rein> (accessed: 01.04.22).
- Lowman, M. D. (1992). Leaf Growth Dynamics and Herbivory in Five Species of Australian Rain-Forest Canopy Trees. *Journal of Ecology*, 80. doi: 10.2307/2260689.
- Lønvik, K. & Koksvik, J. I. (1990). Some observations on seasonal variation of radio-caesium contamination in trout (*Salmo trutta* L.) and arctic char (*Salvelinus alpinus* (L.)) in a Norwegian lake after the Chernobyl fall-out. *Hydrobiologia*, 190 (2): 121-125. doi: 10.1007/BF00014102.
- Macdonald, C. R., Elkin, B. T. & Tracy, B. L. (2007). Radiocesium in caribou and reindeer in northern Canada, Alaska and Greenland from 1958 to 2000. *Journal of Environmental Radioactivity*, 93: 1-25. doi: 10.1016/j.jenvrad.2006.11.003.
- Marchinton, R. L. & Hirth, D. H. (1984). Behavior. In Halls, L. K. (ed.) *White-tailed deer: ecology and management*: Harrisburg, PA: Stackpole Books.
- Miljødirektoratet. (2021). *Tsjernobyl-ulykken og Norge*: Miljødirektoratet (accessed: 03.04.22).

- Mousseau, T. A. & Møller, A. P. (2014). Genetic and Ecological Studies of Animals in Chernobyl and Fukushima. *Journal of Heredity*, 105 (5): 704-709. doi: 10.1093/jhered/esu040.
- Møller, A. P. & Mousseau, T. A. (2013). The effects of natural variation in background radioactivity on humans, animals and other organisms. *Biological Reviews*, 88: 226-254. doi: 10.3390/life11060549.
- Naturlig forekommende ioniserende stråling*. (2016). Folkehelseinstituttet (FHI). Available at: <https://www.fhi.no/ml/miljo/straling/mer-om-straling/naturlig-forekommende-ioniserende-straling/> (accessed: 10.02.22).
- NGU (Geological Survey of Norway). (2012). *NGU Geoscience Data Service*. Available at: <https://geo.ngu.no/geoscienceportalopen/Results?minLong=5&maxLong=52&minLat=50&maxLat=82>.
- Nikouee, K. (2021). *Biodistribution of radionuclides in reindeer from Vågå, Norway*. Master thesis: Norwegian University of Life Sciences.
- NRC (National Research Council). (2012). *Exposure Science in the 21st Century: A Vision and a Strategy*. Washington, DC: The National Academic Press.
- NVE (Norges vassdrags- og energidirektorat). (2020). *Flom- og jordskredåret 2019: Norges vassdrags- og energidirektorat*. Available at: <https://www.varsom.no/nytt/nyheter-flom-og-jordskred/flom-og-jordskredaret-2019/> (accessed: 09.04.22).
- Offenbacher, E. L. & Colbeck, S. C. (1991). *Remote sensing of snow covers using the gamma-ray technique*, 91-9: U.S. Army Corps of Engineers. Cold Regions Research & Engineering Laboratory.
- Oosenbrug, S. M. & Theberge, J. B. (1980). Altitudinal Movements and Summer Habitat Preferences of Woodland Caribou in the Kluane Ranges, Yukon Territory. *Arctic*, 33: 59-72.
- Oughton, D. H., Strømman, G. & Salbu, B. (2013). Ecological risk assessment of Central Asian mining sites: application of the ERICA assessment tool. *J Environ Radioact*, 123: 90-98. doi: 10.1016/j.jenvrad.2012.11.010.
- Ozasa, K., Grant, E. J. & Kodama, K. (2018). Japanese Legacy Cohorts: The Life Span Study Atomic Bomb Survivor Cohort and Survivors' Offspring. *Journal of Epidemiology*, 28 (4): 162-169. doi: 10.2188/jea.JE20170321.
- Pedersen, B. (2021). *Berlinerblått: Store norske leksikon*. Available at: <https://snl.no/berlinerbl%C3%A5tt> (accessed: 14.01.22).
- Pop, I. M., Bereczky, L., Chiriac, S., Iosif, R., Nita, A., Popescu, V. D. & Rozyłowicz, L. (2018). Movement ecology of brown bears (*Ursus arctos*) in the Romanian Eastern Carpathians. *Nature Conservation*, 26 (26): 15-31. doi: 10.3897/natureconservation.26.22955.
- Punsvik, T., Frøstrup, J. C. & Benberg, B. (2016). *Villreinen : fjellviddas nomade : biologi, historie, forvaltning*. Arendal: Friluftsførl.
- Ravna, Ø. & Benjaminsen, T. A. (2018). *Reindrif: Store norske leksikon*. Available at: <https://snl.no/reindrif> (accessed: 14.01.22).
- Saito, K., Ishigure, N., Petoussi-Henss, N. & Schlattl, H. (2012). Effective dose conversion coefficients for radionuclides exponentially distributed in the ground. *Radiat Environ Biophys*, 51: 411-423. doi: 10.1007/s00411-012-0432-y.
- Salbu, B., Skipperud, L. & Lind, O. C. (2015). Sources Contributing to Radionuclides in the Environment: With Focus on Radioactive Particles. In Walther, C. & Gupta, D. K. (eds) *Radionuclides in the Environment - Influence of chemical speciation and plant uptake on radionuclide migration*, pp. 1-36: Springer International Publishing.
- Sato, I., Sasaki, J., Satoh, H., Deguchi, Y., Otani, K. & Okada, K. (2015). Distribution of radioactive cesium and its seasonal variations in cattle living in the "difficult-to-return zone" of the Fukushima nuclear accident. *Animal Science Journal*, 87 (4): 607-611. doi: 10.1111/asj.12463.
- Silverman, B. W. (1986). *Density estimation for statistics and data analysis*: Chapman and Hall.
- Skarin, A. & Åhman, B. (2014). Do human activity and infrastructure disturb domesticated reindeer? The need for the reindeer's perspective. *Polar biology*, 37 (7): 1041-1054. doi: 10.1007/s00300-014-1499-5.
- Skogland, T. (1984). Wild reindeer foraging-niche organization. *Ecography (Copenhagen)*, 7 (4): 345-379. doi: 10.1111/j.1600-0587.1984.tb01138.x.

- Skuterud, L., Ytre-Eide, M. A., Hevrøy, T. H. & Thørring, H. (2016). *Caesium-137 in Norwegian reindeer and Sámi herders – 50 years of studies*. II International Conference on Radioecological Concentration Processes: II International Conference 50 years later, Seville, Spain.
- Smith, M. L., Taylor, H. W. & Sharma, H. D. (1993). Comparison of the post-Chernobyl <sup>137</sup>Cs contamination of mushrooms from eastern Europe, Sweden, and North America. *Appl Environ Microbiol*, 59 (1): 134-139. doi: 10.1128/AEM.59.1.134-139.1993.
- Statens kartverk. (2007). *Toporaster WMS*. Available as a web map service (WMS) at: <http://openwms.statkart.no/skwms1/wms.toporaster4>.
- Strand, P. (1994). *Radioactive fallout in Norway from the Chernobyl accident. Studies on the behaviour of radiocaesium in the environment and possible health impacts*: Norwegian Radiation Protection Authority.
- Sugiyama, H., Takahashi, M. N., Terada, H., Kuwahara, C., Maeda, C., Anzai, Y. & Kato, F. (2008). Accumulation and Localization of Cesium in Edible Mushroom (*Pleurotus ostreatus*) Mycelia. *J. Agric. Food Chem*, 56 (20): 9641-9646. doi: 10.1021/jf801269t.
- Suliman, I. I. & Alsafi, K. (2021). Radiological Risk to Human and Non-Human Biota Due to Radioactivity in Coastal Sand and Marine Sediments, Gulf of Oman. *Life*, 11 (6): 549. doi: 10.3390/life11060549.
- Suter, G. W. & Barnthouse, L. W. (2007). *Ecological risk assessment*. 2nd. ed. Boca Raton, FL: CRC Press.
- Thørring, H., Baranwal, V. C., Ytre-Eide, M. A., Rønning, J. S., Muring, A., Stampolidis, A., Drefvelin, J., Watson, R. J. & Skuterud, L. (2019). Airborne radiometric survey of a Chernobyl-contaminated mountain area in Norway – using ground-level measurements for validation. *J Environ Radioact*, 208-209: 106004-106004. doi: 10.1016/j.jenvrad.2019.106004.
- Ulanovsky, A. (2014). Absorbed doses in tissue-equivalent spheres above radioactive sources in soil. *Radiation and Environmental Biophysics*, 53: 729-737. doi: 10.1007/s00411-014-0561-6.
- UNSCEAR (United Nations Scientific Committee on the Effects of Atomic Radiation). (2010). *Sources and Effects of Ionizing Radiation. 2008 Report to the General Assembly with Scientific Annexes. Volume I*. New York: United Nations Scientific Committee on the Effects of Atomic Radiation.
- van Beest, F. M., Rivrud, I. M., Loe, L. E., Milner, J. M. & Mysterud, A. (2011). What determines variation in home range size across spatiotemporal scales in a large browsing herbivore? *J Anim Ecol*, 80 (4): 771-785. doi: 10.1111/j.1365-2656.2011.01829.x.
- Velle, W. M. (2020). *Nedføring*: Store norske leksikon. Available at: <https://snl.no/nedf%C3%B4ring> (accessed: 14.01.22).
- Vistnes, I. & Nellemann, C. (2007). Impacts of human activity on reindeer and caribou: The matter. *Rangifer*, 27 (3): 47. doi: 10.7557/2.27.3.269.
- Walker, C. H., Sibly, R. M., Hopkin, S. P. & Peakall, D. B. (2012). *Principles of Ecotoxicology*. 4 ed. Florida (USA): CRC Press.
- Zhao, X., Wang, W.-X., Yu, K. N. & Lam, P. K. S. (2001). Biomagnification of radiocesium in a marine piscivorous fish. *Marine Ecology Progress Series*, 222: 227-237. doi: 10.3354/meps222227.
- Zhu, Y. G. & Smolders, E. (2000). Plant uptake of radiocaesium: a review of mechanisms, regulation and application. *J. Exp. Bot*, 51 (351): 1635-1645. doi: 10.1093/jexbot/51.351.1635.
- Aarkrog, A. (2003). Input of anthropogenic radionuclides into the World Ocean. *Deep Sea Research Part II: Tropical Studies in Oceanography*, 50 (17-21): 2597-2606. doi: 10.1016/S0967-0645(03)00137-1.

## Appendix

### Appendix A

#### Method Calculations and Formulas

##### A.1. Calculation of Conversion Factor for %K

When 0.0117% of K present in soil is radioactive potassium ( $^{40}\text{K}$ ) and the activity concentration of  $^{40}\text{K}$  is  $2.617 \cdot 10^5$  Bq/g, then:

$$\% K * 10 = \frac{g K}{kg soil}$$

$$\frac{g K}{kg soil} * 0.000117 = \frac{g ^{40}K}{kg soil}$$

$$\frac{g ^{40}K}{kg soil} * (2.617 * 10^5) = \frac{Bq ^{40}K}{kg soil}$$

Using 1% K to find the conversion factor used to convert from %K to the activity concentration of  $^{40}\text{K}$  in soil:

$$1\% K * 10 = \frac{10 g K}{kg soil}$$

$$\frac{10 g K}{kg soil} * 0.000117 = \frac{0.00117 g ^{40}K}{kg soil}$$

$$\frac{0.00117 g ^{40}K}{kg soil} * (2.617 * 10^5) = \frac{306 Bq ^{40}K}{kg soil}$$

##### A.2. Calculations of Conversion Factor for kBq/m<sup>2</sup> $^{137}\text{Cs}$

When soil density is  $1.6 \text{ g/cm}^3$ , a 3 cm deep layer of soil corresponds to a mass depth of 48 kg/m<sup>2</sup>, then:

$$\frac{1 kBq ^{137}Cs}{m^2} = \frac{1 kBq ^{137}Cs}{48 kg soil} = \frac{1000 Bq ^{137}Cs}{48 kg soil}$$

$$\frac{1000 Bq ^{137}Cs}{48 kg soil} : 48 = \frac{\frac{1000}{48} Bq ^{137}Cs}{kg soil} = \frac{20.8 Bq ^{137}Cs}{kg soil}$$

### A.3. Calculation of Combined Uncertainty GPS-Dosimeter Measurements

The combined uncertainty ( $u_c$ ) includes all uncertainty components quantified, here represented as standard deviations ( $\sigma$ ). Uncertainties of dosimeter measurements, internal  $^{137}\text{Cs}$  activity concentration, and K-mapping are all included in the combined uncertainty for the corrected GPS-dosimeter measurements for each reindeer.

$$u_c = \sqrt{(\sigma_{dosimeter})^2 + (\sigma_{internal\ ^{137}Cs})^2 + (\sigma_{mapping\ of\ K})^2}$$

## Appendix B

### Home Range and Core Area Properties

**Table 8:** Average altitude (m) in home range and core area for each of the three reindeer.

Average altitude (m)	37403	37404	37405
Home range	1359	1293	1311
Core area	1418	1330	1363

**Table 9:** Five  $^{137}\text{Cs}$  contamination zones ( $\text{kBq}/\text{m}^2$ ) with associated proportion of home range and core area for reindeer 37403, based on  $^{137}\text{Cs}$  concentration maps from NGU (Geological Survey of Norway).

$^{137}\text{Cs}$ contamination zone ( $\text{kBq}/\text{m}^2$ )	Home range		Core area	
	Zone's proportion of home range (%)	Median $^{137}\text{Cs}$ in zone ( $\text{kBq}/\text{m}^2$ )	Zone's proportion of core area (%)	Median $^{137}\text{Cs}$ in zone ( $\text{kBq}/\text{m}^2$ )
0-20	19.1	14.1	16.5	13.0
20-40	57.0	30.0	44.2	30.5
40-60	19.9	45.9	37.0	47.5
60-80	3.5	65.4	2.3	62.6
>80	0.5	85.4	0.1	80.9

**Table 10:** Five  $^{137}\text{Cs}$  contamination zones ( $\text{kBq}/\text{m}^2$ ) with associated proportion of home range and core area for reindeer 37404, based on  $^{137}\text{Cs}$  concentration maps from NGU (Geological Survey of Norway).

$^{137}\text{Cs}$ contamination zone ( $\text{kBq}/\text{m}^2$ )	Home range		Core area	
	Zone's proportion of home range (%)	Median $^{137}\text{Cs}$ in zone ( $\text{kBq}/\text{m}^2$ )	Zone's proportion of core area (%)	Median $^{137}\text{Cs}$ in zone ( $\text{kBq}/\text{m}^2$ )
0-20	22.0	13.7	10.4	15.7
20-40	53.6	29.5	56.8	30.5
40-60	20.6	46.8	24.5	47.5
60-80	3.4	65.1	7.6	65.7
>80	0.4	84.9	0.7	83.6



**Table 11:** Five  $^{137}\text{Cs}$  contamination zones ( $\text{kBq}/\text{m}^2$ ) with associated proportion of home range and core area for reindeer 37405, based on  $^{137}\text{Cs}$  concentration maps from NGU (Geological Survey of Norway).

$^{137}\text{Cs}$ contamination zone ( $\text{kBq}/\text{m}^2$ )	Home range		Core area	
	Zone's proportion of home range (%)	Median $^{137}\text{Cs}$ in zone ( $\text{kBq}/\text{m}^2$ )	Zone's proportion of core area (%)	Median $^{137}\text{Cs}$ in zone ( $\text{kBq}/\text{m}^2$ )
0-20	21.7	13.9	12.4	15.1
20-40	54.2	29.2	47.5	29.9
40-60	20.3	46.8	30.0	49.4
60-80	3.3	65.1	9.7	64.9
>80	0.4	84.9	0.5	83.3

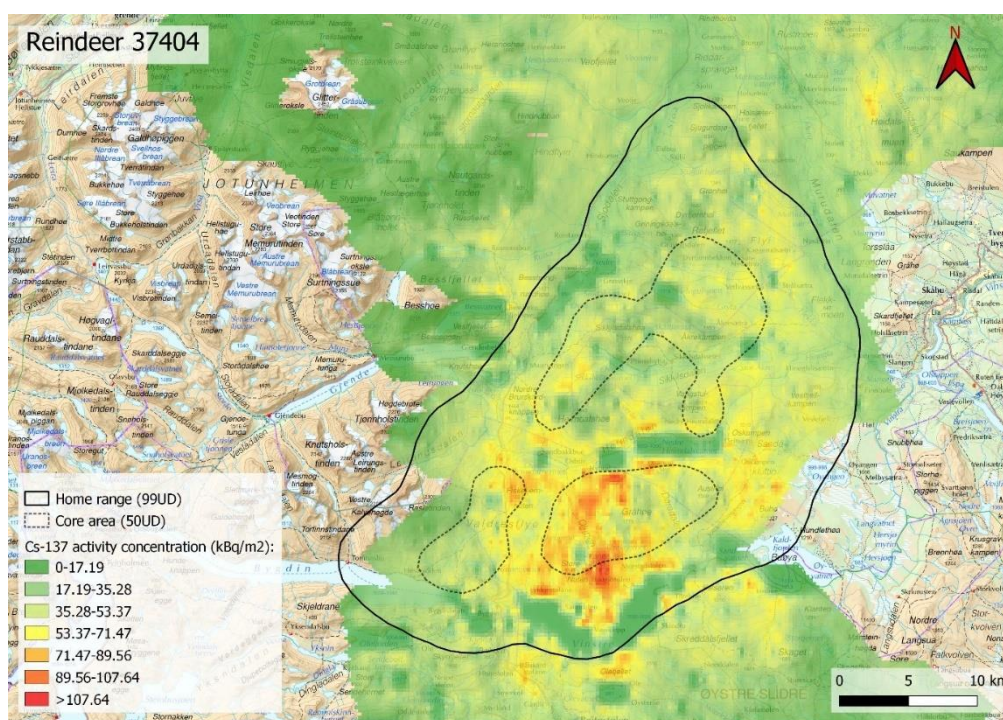


**Figure 17:** Contamination levels of  $^{137}\text{Cs}$  in home range and core area for reindeer 37404 in 2016. Mapdata derived from: 1) Statens kartverk. (2007). Toporaster WMS. Available as a web map service (WMS) at: <http://openwms.statkart.no/skwms1/wms.toporaster4>, 2) NGU (Geological Survey of Norway). (2020). Unpublished.

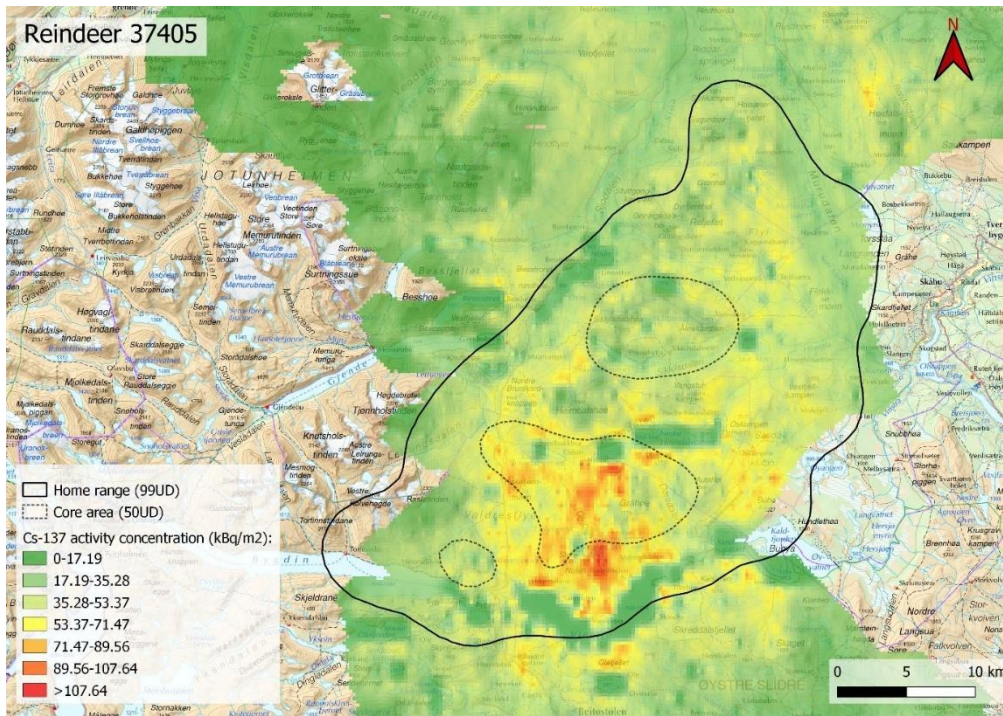


**Figure 18:** Contamination levels of  $^{137}\text{Cs}$  in home range and core area for reindeer 37405 in 2016. Map data derived from: 1) Statens kartverk. (2007). Toporaster WMS. Available as a web map service (WMS) at: <http://openwms.statkart.no/skwms1/wms.toporaster4>, 2) NGU (Geological Survey of Norway). (2020). Unpublished.



**Norges miljø- og biovitenskapelige universitet**  
Noregs miljø- og biovitenskapelige universitet  
Norwegian University of Life Sciences

Postboks 5003  
NO-1432 Ås  
Norway